RADAR Signal Processing using Multi-Objective Optimization Techniques

Vinod Kumar
Roll no. 213EC6256

Department of Electronics and Communication Engineering
National Institute of Technology, Rourkela
Rourkela, Odisha, India
2015

RADAR Signal Processing using Multi-Objective Optimization Techniques

Thesis submitted in partial fulfillment of the requirements for the degree of

Master of Technology

in

Signal & Image Processing

by

Vinod Kumar

Roll no. 213EC6256

under the guidance of

Prof. Ajit Kumar Sahoo

Department of Electronics and Communication Engineering

National Institute of Technology, Rourkela

Rourkela, Odisha, India

2015

dedicated to my parents...

National Institute of Technology
Rourkela

CERTIFICATE

This is to certify that the work in the thesis entitled **"RADAR Signal Processing using Multi-Objective Optimization Techniques"** submitted by ***Vinod Kumar*** is a record of an original work carried out by him under my supervision and guidance in partial fulfillment of the requirements for the award of the degree of **Master of Technology** in **Signal & Image Processing** from National Institute of Technology, Rourkela. Neither this thesis nor any part of it, to the best of my knowledge, has been submitted for any degree or academic award elsewhere.

Prof. Ajit Kumar Sahoo
Assistant Professor
Department of ECE
National Institute of Technology
Rourkela

National Institute of Technology
Rourkela

DECLARATION

I certify that

1. The work contained in the thesis is done by myself under the supervision of my supervisor.
2. The work has not been submitted to any other Institute for any degree or diploma.
3. Whenever I have used materials (data, theoretical analysis, and text) from other sources, I have given due credit to them by citing them in the text of the thesis and giving their details in the references.
4. Whenever I have quoted written materials from other sources, I have put them under quotation marks and given due credit to the sources by citing them and giving required details in the references.

Vinod Kumar

Acknowledgment

This work is one of the most important achievements of my career. Completion of my project would not have been possible without the help of many people, who have constantly helped me with their full support for which I am highly thankful to them.

First of all, I would like to express my gratitude to my supervisor **Prof. Ajit Kumar Sahoo**, who has been the guiding force behind this work. I want to thank him for giving me the opportunity to work under him. He is not only a good Professor with deep vision but also a very kind person. I consider it my good fortune to have got an opportunity to work with such a wonderful person.

I am obliged to **Prof. K.K. Mahapatra**, HOD, Department of Electronics and Communication Engineering for creating an environment of study and research. I am also thankful to Prof. A.K. Swain, Prof. L.P. Roy, Prof. S. Meher, Prof. S. Maiti, Prof. D.P. Acharya and Prof. S. Ari for helping me how to learn. They have been great sources of inspiration.

I would like to thank all faculty members and staff of the ECE Department for their sympathetic cooperation. I would also like to make a special mention of the selfless support and guidance I received from PhD Scholar Mr. Sanand Kumar and Mr. Nihar Ranjan Panda during my project work.

When I look back at my accomplishments in life, I can see a clear trace of my family's concerns and devotion everywhere. My dearest mother, whom I owe everything I have achieved and whatever I have become; my beloved late father, who always believed in me and inspired me to dream big even at the toughest moments of my life; and sisters; who were always my silent support during all the hardships of this endeavor and beyond.

Vinod Kumar

Abstract

Pulse compression technique is used in radar system to achieve the range resolution of short duration pulses and Signal to Noise Ratio (SNR) of long duration pulses. In pulse compression technique a long duration pulse is transmitted with either a frequency or phase modulation. At receiver end, we use matched filter, which accumulate the energy of long pulse into a short pulse. Linear Frequency Modulated (LFM) pulse is one type of signal used in radar. The matched filter response of LFM pulse gives side lobe of about $-13\,dB$, which can be improved by using windowing, adaptive filtering and optimization techniques. In wide-band radar, for good range resolution, very wide bandwidth is used. The conventional hardware may not be able to sustain this large bandwidth. So the wide-band signal is split into narrow-band signals. These narrow-band signals are transmitted and recombined coherently at receiver's end.

In narrow-band signals, frequency changes linearly for complete duration of pulse. We change the center frequency of each LFM pulse by introducing a frequency step between consecutive pulses. Resultant signal is known as Stepped Frequency Pulse Train (SFPT) or Synthetic Wide-band Waveform (SWW). The disadvantage of SFPT is that when the product of pulse duration and frequency step become more than one, the Autocorrelation Function (ACF) of SFPT yields undesirable peaks, known as grating lobes. Along with grating lobe, the higher peak side lobe either can hides the small targets or can cause the false alarm detection. Also the wide main lobe width deteriorate the range resolution capability of the signal. Many analytic techniques have been proposed in the literature to select the SFPT parameter to suppress the grating lobe, without paying much attention to side lobe and main lobe width. Multi-Objective Optimization (MOO) methods are also used for this purpose.

In this work we compare three MOO algorithms to find the optimized parameter of SFPT. The optimization problem is studied in two ways: In first we take

objective of minimization of grating lobes and peak side lobe level. The constraint is of increase in bandwidth. In second problem, our aim is to minimize the main lobe width, which improves the resolution. The objective functions for second problem are minimization of main lobe width and peak side lobe level. We don't want high grating lobe amplitude, so we add a constraint, which restrict the maximum grating lobe amplitude below a threshold value. Simulations are carried out for different range of parameter values and the simulation result shows the potential of the MOO approach.

Keywords: ACF, Grating Lobes, Matched filter, Multi-objective optimization, Pulse Compression, Side lobes.

Contents

List of Figures

List of Tables

List of Algorithms

List of Acronyms

Acronym	Description
ACF	Autocorrelation Function
AF	Ambiguity Function
AWGN	Additive White Gaussian Noise
BW	Bandwidth
IDEA	Infeasibility Driven Evolutionary Algorithm
CW	Continuous Wave
LFM	Linear Frequency Modulation
NSGA	Nondominated Sorting Genetic Algorithm
MOO	Multi-Objective Optimization
MOPSO	Multi-Objective Particle Swarm Optimization
PCR	Pulse Compression Ratio
PSD	Power Spectral Density
PSO	Particle Swarm Optimization
PSR	Peak to Side lobe Ratio
RADAR	Radio Detection and Ranging
SFPT	Stepped Frequency Pulse Train
SNR	Signal to Noise Ratio

Chapter 1

Thesis Overview

Background

Motivation

Objective

Thesis Organization

Chapter 1

Thesis Overview

1.1 Background

From last few decades, radar system is widely used in many applications like military and commercial. The reason for the widespread use of radar is advancement in the signal generation and processing technology. In military applications, high range resolution radar systems are always a top priority. High range resolution radar design is hindered by the high bandwidth requirement.

Applying modulation is one way to increase the bandwidth of the signal. Linear frequency modulated (LFM) pulse is one such signal that gives us good range resolution. Range resolution can be further improved by using Stepped Frequency Pulse Train (SFPT). The SFPT employ inter-pulse, pulse compression technique. In this technique, a frequency step, Δf, is applied to consecutive pulses. Because of frequency step, carrier frequency changes linearly. Applying frequency step Δf, on the successive pulse, increase the signal bandwidth. The bandwidth of SFPT become equal to the product of number of coherently integrated pulse, N, and a frequency step size, Δf. SFPT overall become a wide-band signal, but each pulse is a narrow-band signal. This feature makes the design of receiver simpler.

The key advantage of the SFPT as compared to other radar signal is its high range resolution with wide overall bandwidth and small instantaneous bandwidth. Implementation of SFPT is simple. The disadvantage of SFPT is that it exhibits high side lobe at location $\tau_g = g/\Delta f$. These side lobes, known as grating lobes, have comparable energy as to main lobe. Grating lobe in some applications can hide the weak target or can cause a false alarm, so they are not desirable in the

output. Also when we improve the range resolution of a pulse, its main lobe width decreases. From the properties of ambiguity function, if we try to squeeze the main lobe, the volume removed from the main lobe must appear somewhere else. This volume appears in the form of side lobes. So the better the range resolution, the more side lobes it shows. These side lobes are also not desirable. Proper selection of the parameter of SFPT can yield an optimum range resolution with suppressed or no grating low and minimized peak side lobe.

1.2 Motivation

Many efforts have been made, in the available literature, to suppress the side lobes in the matched filter output of the radar system. Different mismatch filters are proposed in past to improve the peak to side lobe ratio, but the mismatched filters provide weak convergence performance. So there is a need to improve the mismatch filters.

In polyphase and LFM waveforms, amplitude weighing techniques can be used to suppress side lobes. When there is Doppler shift in the waveform, the matched filter gives us degraded PSR. Under such situations, it is required to improve the PSR.

The matched filter output for stepped frequency LFM pulse train is its auto-correlation function. Stepped frequency pulse train shows the grating lobe in the matched filter output. Grating lobe appears because of a constant frequency step. Many techniques are available in the literature to suppress the grating lobe, but they ignore the PSR and main lobe width. Therefore, there is a need to develop methods by which we can choose the parameters of stepped frequency waveform such that it provides high range resolution, lower grating lobes and reduced side lobes.

1.3 Objective

The objective of this work is to find out the optimum parameter of stepped frequency pulse train, which can yield good range resolution with suppressed or

eliminated grating lobe. With grating lobe suppression, we also aims for the minimization of the peak side lobe. In the radar system, if we try to suppress or eliminate the grating lobe, then the peak side lobe might increase (From ambiguity function property). For us, both side lobes and grating lobe are undesired. We want to eliminate both grating lobe and side lobe.

Here we have a conflicting situation, minimizing grating lobe result in increased side lobe. To deal with this situation we use Multi-Objective Optimization (MOO) techniques. MOO techniques used to simultaneously optimized one or more than one objective function. In this work, we use NSGA-II, MOPSO and IDEA algorithms to find the optimized parameter of stepped frequency pulse train which can give us good range resolution, minimum grating lobe amplitude, and low peak side lobe.

1.4 Thesis Organization

1. **Chapter 1: Thesis Overview**

2. **Chapter 2: Introduction**
   This chapter introduces the basics concept of pulse compression, matched filter, ambiguity functions and various signals used in radar. MATLAB simulation of some signals with their ambiguity function is also presented in this chapter.

3. **Chapter 3: Coherent Train of LFM Pulses**
   In this chapter, we discussed about the Coherent Train of LFM Pulses (stepped frequency pulse train). We, first derived the expression for ACF of SFPT, then grating lobe and side lobes are explained. Literature review for side lobe and grating lobe is presented next. Problem used for optimization is formulated in the next section and finally the conclusion for the chapter is presented.

4. **Chapter 4: Multi-Objective Optimization**
   Multi-objective optimization techniques are discussed in this section. The basic concept is presented first. Then we discuss the MOO techniques used to find the optimized parameter of SFPT. In MOO techniques, first we discuss

the Nondominated Sorting Genetic algorithm (NSGA-II), then Multi-Objective Particle Swarm Optimization (MOPSO) and at last Infeasibility Driven Evolutionary Algorithm (IDEA) is discussed. Simulation of some standard test problem is done for all three optimization algorithms. In last section conclusion for the chapter is presented.

5. **Chapter 5: Simulation Results**
   This chapter presents the simulation results for the problem formulated in chapter 3. MATLAB simulation using MOO algorithms for both problems are shown for various values of signal parameters. Results obtain using MOO algorithms is also compared on the basis of a performance comparison metrics.

6. **Chapter 6: Conclusion and Future Work**
   In this chapter the conclusion of this work is presented. This chapter also gives details about the further research work which can be attempted subsequently.

Chapter 2

Introduction

Introduction

Pulse Compression

Matched Filter

Ambiguity Function

Radar Signals

Simulation Results

Conclusion

Chapter 2
Introduction

2.1 Introduction

RADAR is an acronym of RAdio Detection And Ranging. Radar is used in many applications to find the presence of an object within the search space. Apart from just giving the existence of the object, modern radars are capable of providing many other information about the properties of the object like range, altitude, size, direction, speed, etc. The radar antenna transmits an electromagnetic signal into the search space. The transmitted signal is reflected by the object present (if any). Radar antenna receives the reflected signal, known as echo, from the object. The echoes are processed to extract the information about the object. There are two type of radar, Continuous Wave (CW) radar and pulsed radar. The CW radar continuously transmits the signal. CW radar has the advantage of unambiguous Doppler measurement, but it require two antennas. Also due to the continuous nature of the signal the target range measurement of CW radar is ambiguous.

In the modern era, we use pulse radar system because it provides accurate range information. Also, the hardware requirement is less since transmitter and receiver can share the same antenna. The unambiguous range of pulsed radar is given by [1, p. 3]

$$R_u = \frac{cT_r}{2}F \tag{2.1}$$

Where c is the speed of light, T_r is the pulse repetition time. One such pulse with pulse duration T_p is shown in Figure 2.1. The range resolution can be ex-

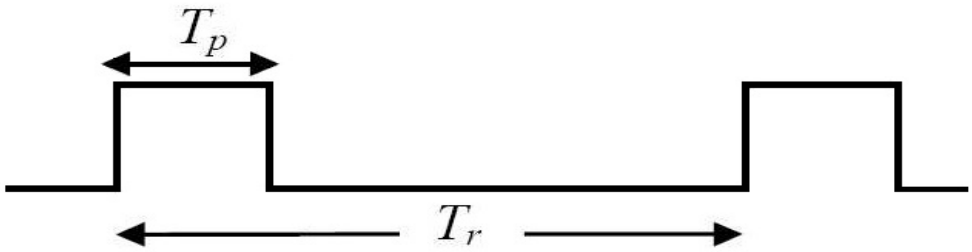

Figure 2.1: Pulsed RADAR waveform

pressed as [2, p. 5], [3]

$$\Delta R = \frac{cT_p}{2} = \frac{c}{2B} \tag{2.2}$$

Here B is for the bandwidth of the pulse. Pulse width decides the range resolution of the signal. Low pulse width gives the better range resolution, but low pulse width decrease the average pulse energy ($P_{avg} = \frac{P_t T_P}{T_r}$) [1, p. 74]. So we have to transmit more power to have reasonable average pulse energy.

The minimum detectable signal to noise ratio is given by [1, p. 34] as

$$\left(\frac{S}{N}\right)_{\min} = \frac{P_t G A_e \sigma}{(4\pi)^2 k T_0 B F_n R_{\max}^4} \tag{2.3}$$

To detect signal, Signal to Noise Ratio (SNR) should be more than $\left(\frac{S}{N}\right)_{\min}$. For constant radar parameter $\left(\frac{S}{N}\right)_{\min}$ is high for high P_t. So we can't detect signals with low SNR when we transmit high power. This is one drawback of using low pulse width.

In Radar system, we have a conflicting problem. We want pulse width to low for good range resolution, but with low pulse width, we have to transmit more power to detect weak signals. To transmit low power(detect low SNR signal) with good range resolution, pulse compression techniques is employed in radar systems.

2.2 Pulse Compression

Equation 2.2 gives the range resolution for a radar signal. The time duration of the unmodulated pulse is inversely proportional to its bandwidth. Low time duration and high bandwidth signal exhibits an excellent range resolution, but we can not increase the bandwidth of the signal (or decrease the time duration)

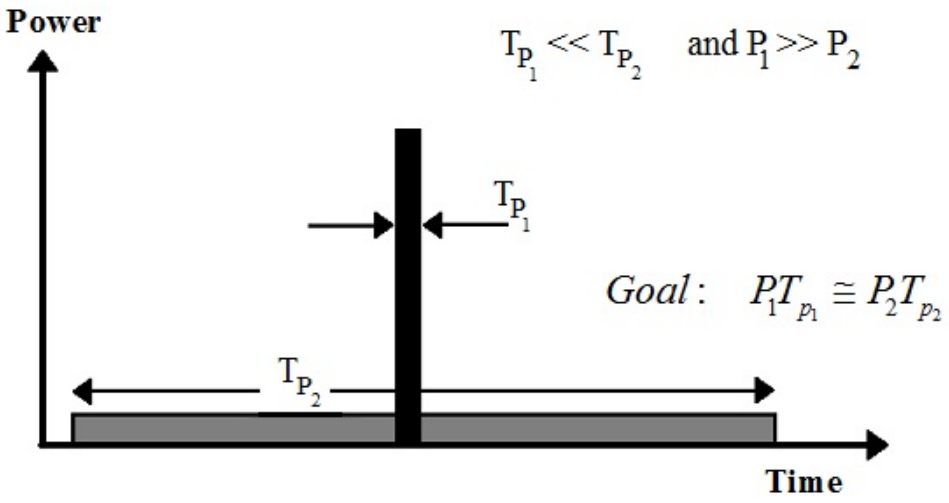

Figure 2.2: Transmitter and receiver ultimate signals

indefinitely. Fourier theory says that, for the signal having bandwidth B, the time period can not become less than $1/B$. In other words, the product of time and bandwidth can not become less than unity. For large distance communication, short duration pulses require high energy. The equipment used in high power radar are bulky, requires more space and they increase the total cost of the system. Therefore, high power transmission is restricted by the transmitter.

The maximum detection range depends upon the energy of the received echo signal. For echo signal to have high energy, transmitted pulse should have high energy. The energy of received echo depends on the pulse duration and peak transmitted power. We can achieve the average power of low pulse width and high peak transmission power by transmitting low peak power with high pulse width. Figure 2.2 shows two such pulse; both are having different pulse width, but their energy is same.

Frequency or phase modulation technique can be used to enhance the bandwidth of a large duration pulse. Increase in bandwidth also improves the range resolution. In pulse compression technique, we transmit low peak power, long duration pulse. This pulse is either phase or frequency modulated. At the receiver side, we pass this received signal through matched filter. Matched filter accumulate the energy of long pulse into a short pulse. The performance of pulse

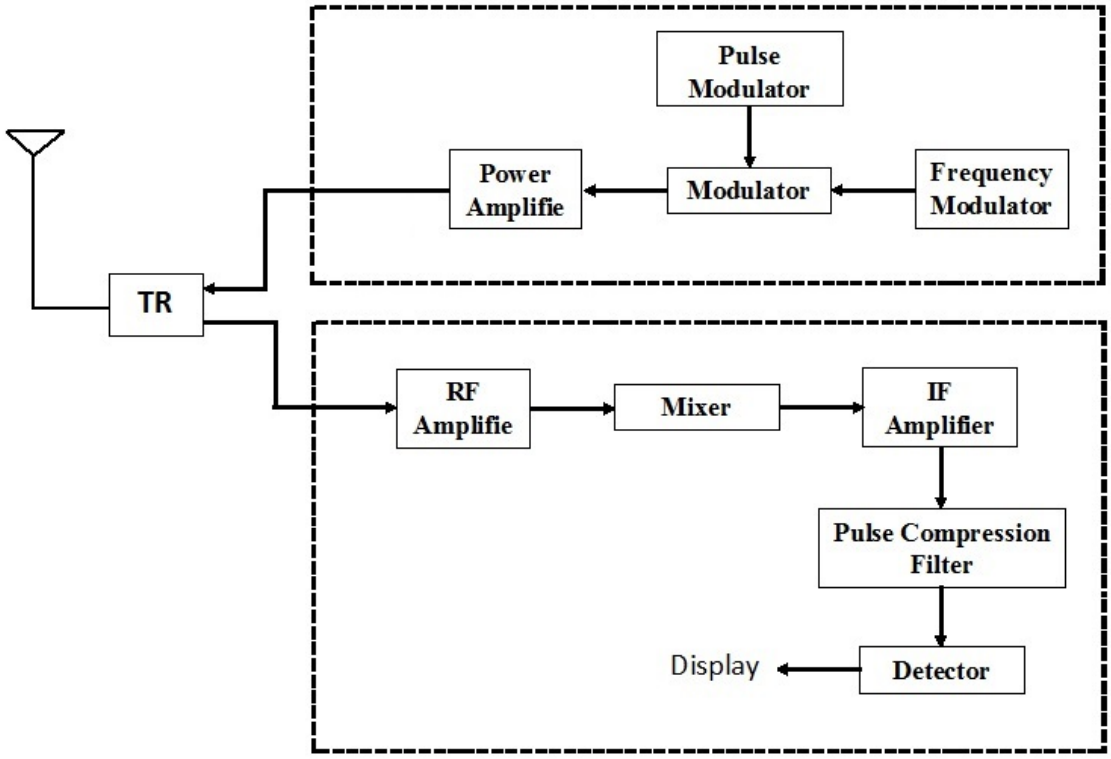

Figure 2.3: Block diagram of a pulse compression radar system

compression is measured by Pulse Compression Ratio (PCR), and it is defined in [1] as

$$PCR = \frac{pulse\ ,width\ before\ compression}{pulse\ width\ after\ compression} \tag{2.4}$$

The higher the value of PCR, the better will be the compression.

Figure 2.3 shows the block diagram of a radar pulse compression system. The transmitted signal is either frequency or phase modulated to enhance the bandwidth. Transceiver (TR) is a switching unit, which helps to use the same antenna as a transmitter and as a receiver. Matched filter is used in pulse compression system at the receiver side. Its frequency spectrum matches with that of transmitted signal. The matched filter gives correlation between two signals (transmitted and received pulses). When we give received pulse as an input to matched filter, then we will get maximum SNR, compressed pulse as an output, if properties of received pulse matches to the transmitted pulse.

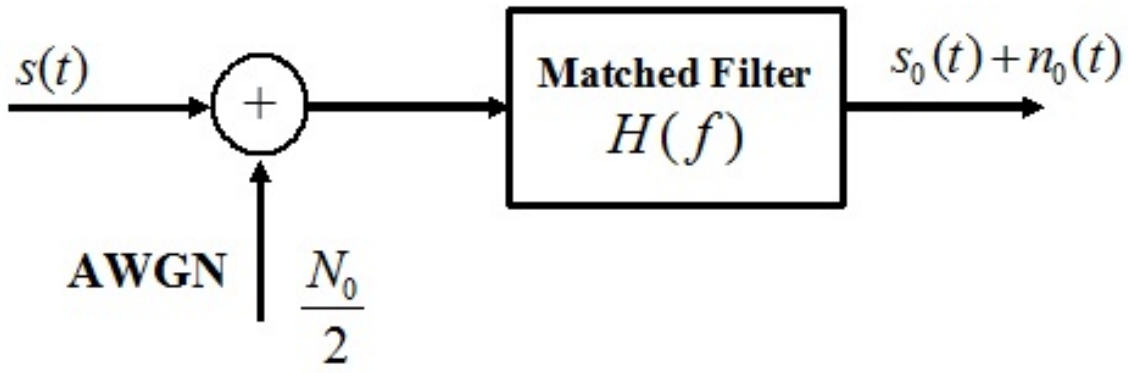

Figure 2.4: Block diagram of a matched filter

2.3 Matched Filter

A radar detects the presence of an object by echo signal reflected from the object. Additive White Gaussian Noise (AWGN) present in search space may corrupts the reflected signal. The noise power in received signal may be comparable with original signal power, which gives us the low value of SNR. The maximum probability of detection depends on the SNR [1, p. 43]. So to maximize SNR, matched filter is employed. The matched filter impulse response is expressed in terms of the signal for which the filter is matched. When the exactly matched signal (plus white noise) is passed to matched filter, it gives maximum SNR [4, p. 20]. The maximum SNR occurs at a particular instant of time. This time is a design parameter.

The block diagram of matched filter is shown in Figure 2.4. An input signal $s(t)$ passes through the channel, which corrupts the signal by adding AWG noise. Let the two-sided Power Spectral Density (PSD) of the AWGN channel is $\frac{N_0}{2}$. We want to find the filter transfer function $H(f)$ which results in maximum SNR at a predetermined time delay t_0. The output SNR of matched filter shown in Figure 2.4 is given by [4, p. 24]

$$\left(\frac{S}{N}\right)_{out} = \frac{|s_0(t_0)|^2}{\overline{n_0^2(t)}} \tag{2.5}$$

where S is signal power and N is output noise power. $s_0(t_0)$ is the value of signal,

at the time instant where we want to maximize the SNR. The mean square value of noise is presented as $\overline{n_0^2(t)}$. Let the Fourier transform of $s(t)$ is $S(f)$. $s_0(t)$ can be obtained as

$$s_0(t) = \int_{-\infty}^{\infty} H(f)S(f)e^{j2\pi ft}df \tag{2.6}$$

The value of $s_0(t)$ at $t = t_0$ is given by

$$s_0(t_0) = \int_{-\infty}^{\infty} H(f)S(f)e^{j2\pi ft_0}df \tag{2.7}$$

The mean square value of noise

$$\overline{n_0^2(t)} = \frac{N_0}{2}\int_{-\infty}^{\infty} |H(f)|^2 df \tag{2.8}$$

Substituting equation 2.7 and 2.8 into 2.5 gives

$$\left(\frac{S}{N}\right)_{out} = \frac{\left|\int_{-\infty}^{\infty} H(f)S(f)e^{j2\pi ft_0}df\right|^2}{\frac{N_0}{2}\int_{-\infty}^{\infty}|H(f)|^2df} \tag{2.9}$$

Using Schwarz inequality the numerator of 2.9 can be written as

$$\left|\int_{-\infty}^{\infty} H(f)S(f)e^{j2\pi ft_0}df\right|^2 \leq \int_{-\infty}^{\infty}|H(f)|^2df\int_{-\infty}^{\infty}S(f)e^{j2\pi ft_0}df \tag{2.10}$$

Equality in equation 2.10 if

$$H(f) = K_1\left[S(f)e^{j2\pi ft_0}\right]^* = K_1S^*(f)e^{-j2\pi ft_0} \tag{2.11}$$

Where K_1 is any arbitrary chosen constant and $*$ is for complex conjugate. Using the relationship of $S(f)$ and $H(f)$ into equation 2.5, which corresponds to maximum SNR

$$\left(\frac{S}{N}\right)_{out} = \frac{\int_{-\infty}^{\infty}|S(f)|^2df}{\frac{N_0}{2}} = \frac{2E}{N_0} \tag{2.12}$$

The energy of finite time signal $s_0(t)$ is given by

$$E = \int_{-\infty}^{\infty} |s(t)|^2 dt = \int_{-\infty}^{\infty} |S(f)|^2 df \tag{2.13}$$

From equation 2.13, it is clear that the maximum SNR depends on the energy of the signal, not on the shape of the signal. Applying inverse Fourier transform on equation 2.11 gives the matched filter impulse response as

$$h(t) = K_1 s^*(t_0 - t) \tag{2.14}$$

This equation says that the impulse response of matched filter is a delayed version of input signal with complex conjugate.

The output at time $t = t_0$ is

$$\begin{aligned} s_0(t_0) &= K_1 \int_{-\infty}^{\infty} S(f)S^*(f)e^{-j2\pi f t_0} e^{j2\pi f t_0} df \\ &= K_1 \int_{-\infty}^{\infty} |S(f)|^2 df \\ &= K_1 E \end{aligned} \tag{2.15}$$

This equation say that at predefined delay $t = t_0$ output is the energy of the signal (assume $K_1 = 1$), regardless of the type of waveform. The output of the matched filter is expressed as

$$\begin{aligned} s_0(t) &= s(t) \otimes h(t) \\ &= \int_{-\infty}^{\infty} s(\tau)h(t-\tau)d\tau \\ &= \int_{-\infty}^{\infty} s(\tau)K_1 s^*(\tau - t + t_0)d\tau \\ &= \int_{-\infty}^{\infty} s(\tau)s^*(\tau - t)d\tau \Big|_{K_1=1, t_0=0} \end{aligned} \tag{2.16}$$

Where $\otimes$ is for linear convolution. The right hand side of equation 2.16 is known as autocorrelation function (ACF) of the input signal $s(t)$.

2.3.1 Matched filter for a narrow bandpass signal

Modern radar generally uses narrow-band signals. The Fourier transform of the baseband signal is centered at a carrier frequency ω_c and covers a frequency band of $2B$. The fundamental representation of baseband signal is [4, p. 20]

$$s(t) = g(t)\cos\left[\omega_c t + \phi(t)\right] \tag{2.17}$$

where $g(t)$ and $\phi(t)$ are the natural envelop and instantaneous phase of the $s(t)$ respectively. Another representation of base band signal is

$$s(t) = g_c(t)\cos\omega_c t - g_s(t)\sin\omega_c t \tag{2.18}$$

where $g_c(t)$ is in-phase component and $g_s(t)$ is quadrature component, expressed as

$$\begin{aligned} g_c(t) &= g(t)\cos\phi(t) \\ g_s(t) &= g(t)\sin\phi(t) \end{aligned} \tag{2.19}$$

$g_c(t)$ and $g_s(t)$ both are bounded by a range of frequency, denoted as W both signals can be viewed as baseband signals.

The complex envelop of $s(t)$ is given by

$$u(t) = g_c(t) + jg_s(t) \tag{2.20}$$

The complex envelop gives another expression to represent the signal

$$s(t) = \mathrm{Re}\left\{u(t)\exp(j\omega_c t)\right\} \tag{2.21}$$

The natural envelop of signal is equal to the magnitude of complex envelop

$$s(t) = |u(t)| \tag{2.22}$$

Putting the value of $|u(t)|$ gives another expression to represent narrow band signal as

$$s(t) = \frac{1}{2}u(t)\exp(j\omega_c t) + \frac{1}{2}u^*(t)\exp(-j\omega_c t) \tag{2.23}$$

Using Equation 2.23 in Equation 2.16 yields [4, p. 29]

$$\begin{aligned} s_0(t) = \tfrac{K_1}{4}\int_{-\infty}^{\infty} &\left[u(\tau)e^{j2\pi f_0\tau} + u^*(\tau)e^{-j2\pi f_0\tau}\right] \\ &\left\{u^*(\tau - t + t_0)e^{-j2\pi f_0(\tau - t + t_0)} + u(\tau - t + t_0)e^{j2\pi f_0(\tau - t + t_0)}\right\} d\tau \end{aligned} \tag{2.24}$$

on performing the cross product, give us

$$\begin{aligned} s_0(t) &= \tfrac{K_1}{4}\exp\left[j\omega_c(t-t_0)\right]\int_{-\infty}^{\infty} u(\tau)u^*(\tau-t+t_0)d\tau \\ &+\tfrac{K_1}{4}\exp\left[-j\omega_c(t-t_0)\right]\int_{-\infty}^{\infty} u^*(\tau)u(\tau-t+t_0)d\tau \\ &+\tfrac{K_1}{4}\exp\left[j\omega_c(t-t_0)\right]\int_{-\infty}^{\infty} u^*(\tau)u^*(\tau-t+t_0)\exp\left(-j2\omega_c\tau\right)d\tau \\ &+\tfrac{K_1}{4}\exp\left[-j\omega_c(t-t_0)\right]\int_{-\infty}^{\infty} u(\tau)u(\tau-t+t_0)\exp\left(j2\omega_c\tau\right)d\tau \end{aligned} \tag{2.25}$$

the second and fourth part of the above equation is complex conjugate of first and third part respectively. So it can be written as

$$\begin{aligned} s_0(t) &= \tfrac{K_1}{2}\mathrm{Re}\left\{\exp\left[j\omega_c(t-t_0)\right]\int_{-\infty}^{\infty} u(\tau)u^*(\tau-t+t_0)d\tau\right\} \\ &+\tfrac{K_1}{2}\mathrm{Re}\left\{\exp\left[j\omega_c(t-t_0)\right]\int_{-\infty}^{\infty} u^*(\tau)u^*(\tau-t+t_0)\exp\left(-j2\omega_c\tau\right)d\tau\right\} \end{aligned} \tag{2.26}$$

second part of Equation 2.26 is Fourier transform of $\int_{-\infty}^{\infty} u^*(\tau)u^*(\tau-t+t_0)$ evaluated at $\omega=\omega_c$. Since $s(t)$ is a narrow band signal and its spectrum is centered around ω_c. So spectrum of its complex envelop signal $u(t)$ is cut well below ω_c, and we can neglect the second term.

$$\begin{aligned} s_0(t) &\approx \tfrac{K_1}{2}\mathrm{Re}\left\{\exp\left[j\omega_c(t-t_0)\right]\int_{-\infty}^{\infty} u(\tau)u^*(\tau-t+t_0)d\tau\right\} \\ &\mathrm{Re}\left\{\left[\tfrac{K_1}{2}\exp\left(-j\omega_c t_0\right)\int_{-\infty}^{\infty} u(\tau)u^*(\tau-t+t_0)d\tau\right]\exp\left(j\omega_c t\right)\right\} \end{aligned} \tag{2.27}$$

Let we define a new complex envelop:

$$u_0(t) = K_u\int_{-\infty}^{\infty} u(\tau)u^*(\tau-t+t_0)d\tau, \qquad K_u = \frac{K_1}{2}\exp\left(-j\omega_c t_0\right) \tag{2.28}$$

Matched filter output can be written as

$$s_0(t) \approx \mathrm{Re}\left\{u_0(t)\exp\left(j\omega_c t\right)\right\} \tag{2.29}$$

Above two equations shows that the output is matched to narrow-band pulse. Passing the complex envelope of $u(t)$ through the matched filter gives the complex

envelop of output $u_0(t)$.

2.4 Ambiguity Function

Ambiguity function (AF) is the output of matched filter when the input to matched filter is received signal with a Doppler shift ν and a time delay τ relative to a nominal value expected by the filter. The AF can be expressed as [4, p. 34]

$$|\chi(\tau,\nu)| = \left| \int_{-\infty}^{\infty} u(t)u^*(t+\tau)\mathrm{e}^{j2\pi\nu t}dt \right| \tag{2.30}$$

Here $u(t)$ represent the complex envelope of the signal. A positive value of τ means target is moving away from the radar reference position. A positive value of ν implies that is moving towards the radar.

2.4.1 Properties of Ambiguity Function

1. **Property 1:** Maximum at $(0,0)$

   $$|\chi(\tau,\nu)| \leq |\chi(0,0)| = (2E)^2 \tag{2.31}$$

   This property says that the AF has a maximum value at the origin, which is the actual location of the target, when the Doppler shift $\nu = 0$. The maximum value is $(2E)^2$, where E is the energy of echo signal.

2. **Property 2:** Constant volume

   $$\int_{-\infty}^{\infty}\int_{-\infty}^{\infty} |\chi(\tau,\nu)|^2 d\tau d\nu = (2E)^2 \tag{2.32}$$

   The total volume under AF is constant and equal to $(2E)^2$.

   From property 1 and 2, we can say that, if we try to squeeze the AF to a narrow peak at origin, then the peak can not exceed the value of $(2E)^2$. Further, the volume removed from the peak must emerge somewhere else [4, p. 35].

3. **Property 3:** Symmetry with respect to the origin

   $$|\chi(-\tau,-\nu)| = |\chi(\tau,\nu)| \tag{2.33}$$

This property says that we only need to study two adjacent quadrants to get complete information about AF.

4. **Property 4:** LFM effect
   Let a complex envelop $u(t)$ has an AF

$$u(t) \Leftrightarrow |\chi(\tau, \nu)| \tag{2.34}$$

   then adding LFM, the AF of resultant signal is given as:

$$u(t)e^{j\pi kt^2} \Leftrightarrow |\chi(\tau, \nu - k\tau)| \tag{2.35}$$

   This property says that adding LFM effect, shears the resulting AF.

2.5 Radar Signals

To get the effect of bandwidth of the low pulse width signal in the high pulse width signal, we apply some kind to modulation to the input signal. Normally phase or frequency modulated signals are used in radar. These two modulated signals are described below.

2.5.1 Phase Modulated Signal

The increase in bandwidth can be achieved by using phase modulation techniques. In phase modulation, we have a pulse of duration T_p. This pulse is divided into N sub-pulses, each of having duration t_b as shown in Figure 2.5. Each sub pulse is assigned with a phase value φ_i, where $i = 1, 2, 3, ...N$. The phase φ_i of sub pulse is selected in accordance with a coding sequence. The basic phase-code modulation technique is binary coding. It requires two phases. The binary code is a sequence of either 0 and 1 or $+1$ and -1. The transmitted signal phase changes between and with respect to the sequence of elements. Since the frequency of transmission is not always a multiple of the reciprocal of the sub pulse interval, hence at the phase reversal points the phase coded signal is usually discontinuous. The PCR of phase coded pulse is obtained as

$$PCR = \frac{T_p}{t_b} \tag{2.36}$$

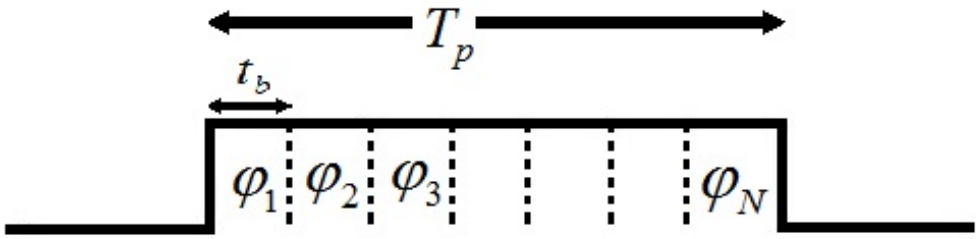

Figure 2.5: Phase modulated waveform

The compression ratio is equivalent to the number of elements in the code, i.e., the number of sub-pulses in the waveform. Matched filter is used at the receiver end to obtain the compressed pulse. The compressed pulse width at the half-amplitude point is usually equal to the width of the sub pulse. Hence, the range resolution is directly proportional to the time duration of one sub pulse of the pulse.

2.5.2 Frequency Modulated Signal

The ACF of the single frequency, unmodulated pulse has a triangular shape. Using this pulse gives very poor range resolution. This is because of the narrow spectrum of the pulse. The pulse spectrum can be widened by using frequency modulation technique. Few frequency modulation techniques are described below:

1. **Linear Frequency Modulation:** LFM modulation is most widely used modulation technique in radar. In this method, the carrier frequency of sinusoidal is varied linearly with time. If the frequency of carrier increases linearly across the pulse, then it is known as up-chirp signal (shown in Figure 2.6), if frequency decreases then it is known as down-chirp signal. The instantaneous phase of chirp signal can be expressed as

$$\varphi(t) = 2\pi(f_0 t + \frac{1}{2}kt^2) \tag{2.37}$$

where f_0 is frequency of the carrier. k is the rate of change of frequency. k is related to the bandwidth B and pulse duration T_p of pulse as

$$k = \frac{B}{T_p} \tag{2.38}$$

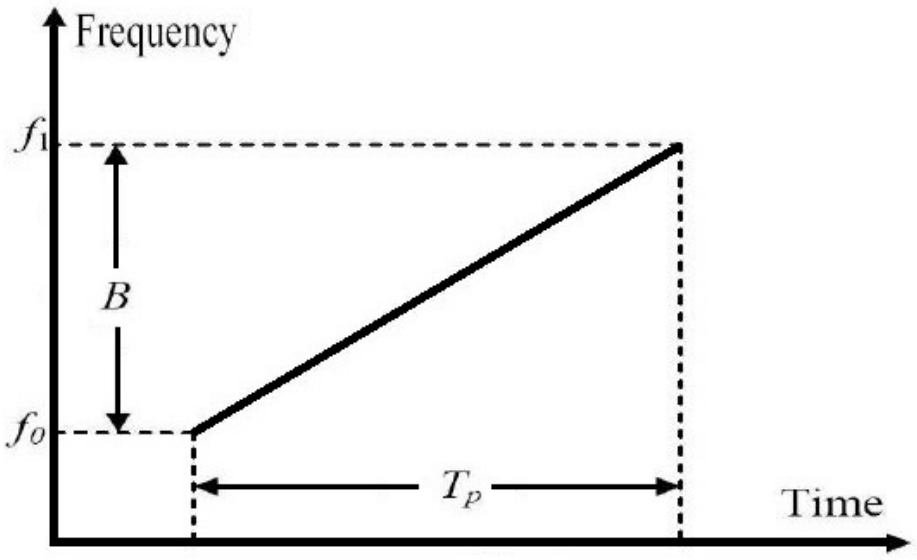

Figure 2.6: The instantaneous frequency of the LFM waveform over time

The instantaneous frequency is given by [4, p. 58]

$$f(t) = \frac{d}{dt}(f_0 t + \frac{1}{2}kt^2) = f_0 + kt \tag{2.39}$$

LFM techniques increase the bandwidth of the signal thereby improving the range resolution by a factor equals to the time-bandwidth product [4, p. 61]. ACF of LFM signal shows high side lobes ($-13.2\ dB$ below the main lobe peak), [1, p. 343] which is not acceptable in certain radar applications where the number of targets are more than one that gives rise to echoes of different amplitudes. Some major techniques like time domain weighting, frequency domain weighting and NLFM are used to get lower side lobes level. The amplitude modulation of the transmitted signal is equivalent to time domain weighting that gives rise to low transmitted power thereby lowering the SNR. Frequency domain weighting broadens main lobe. NLFM overcomes the above two problems, and there is no mismatch loss [2, 5, 6].

2. **Noninear Frequency Modulation:** Despite having several advantages, the nonlinear-FM waveform has little acceptance. The waveform is designed in such a way that it provides the desired amplitude spectrum hence no time or frequency weighting is required in this NLFM waveform for range sidelobe

suppression. The matched filter output, when transmitted signal is an NLFM pulse, gives low side lobe levels. If a weighting is applied to the signal, the resultant loss in SNR can be overcome by the general mismatching techniques. The reduction in frequency side lobes by time weighting a symmetrical FM modulation gives rise to near-ideal ambiguity function [7]. The limitations of the NLFM waveform are listed as:

1. Using NLFM pulse increase the system complexity,
2. There is a very little development of NLFM generation equipments,
3. In NLFM pulse, for each amplitude spectrum, a separate FM modulation design is required.

2.6 Simulation Results

In this section, we simulate the basic waveform used in radar and their ambiguity function. Figure 2.7 and 2.8 shows the plot of LFM pulse. The bandwidth of LFM pulse is $200MHz$ and the pulse duration is $10\mu sec$. Figure 2.7 shows the real part of the pulse and imaginary part of LFM pulse is shown in Figure 2.8. The spectrum of this LFM pulse is shown in Figure 2.9.

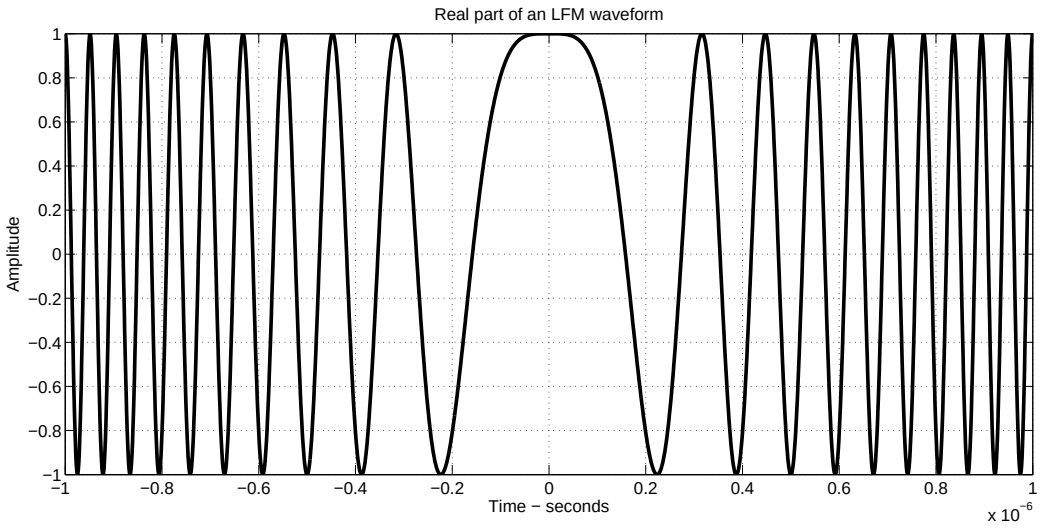

Figure 2.7: Real Part of LFM signal. $B = 200MHz, t = 10\mu$ sec.

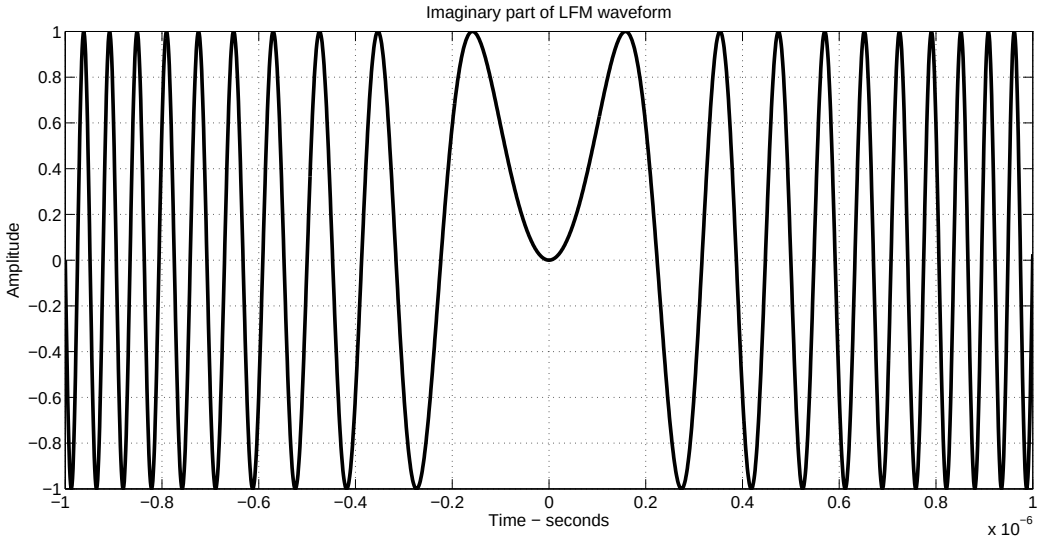

Figure 2.8: Imaginary Part of LFM signal. $B = 200MHz, t = 10\mu\,\mathrm{sec}$.

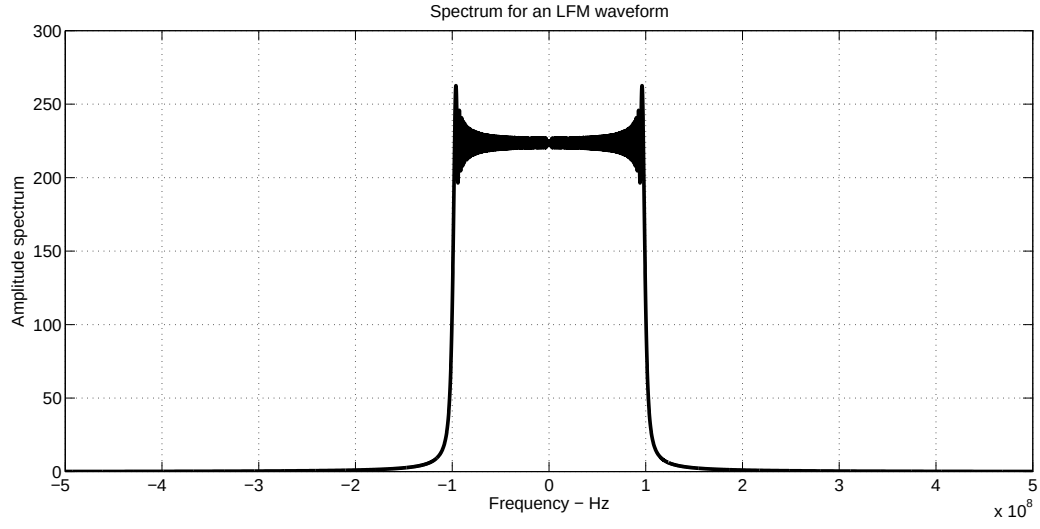

Figure 2.9: Spectrum of LFM signal. $B = 200MHz, t = 10\mu\,\mathrm{sec}$.

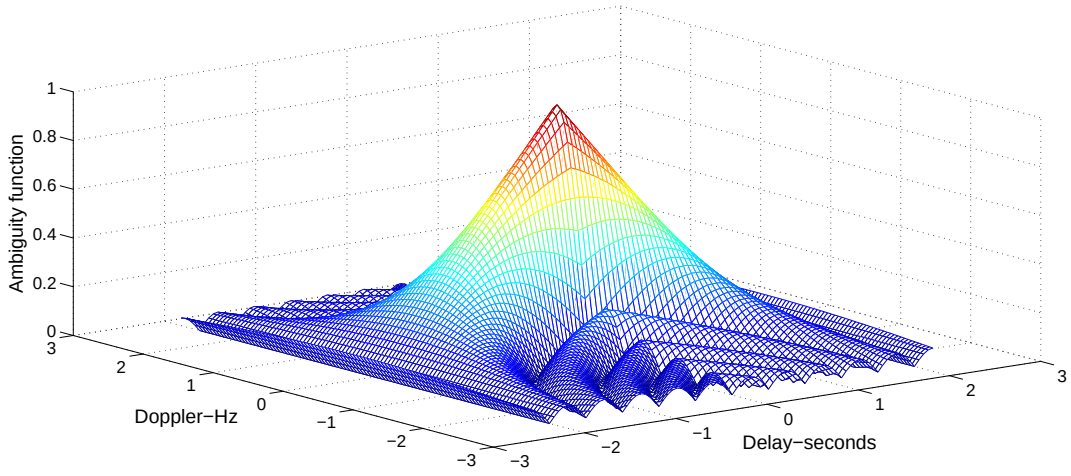

Figure 2.10: Ambiguity function plot of single pulse, constant frequency signal

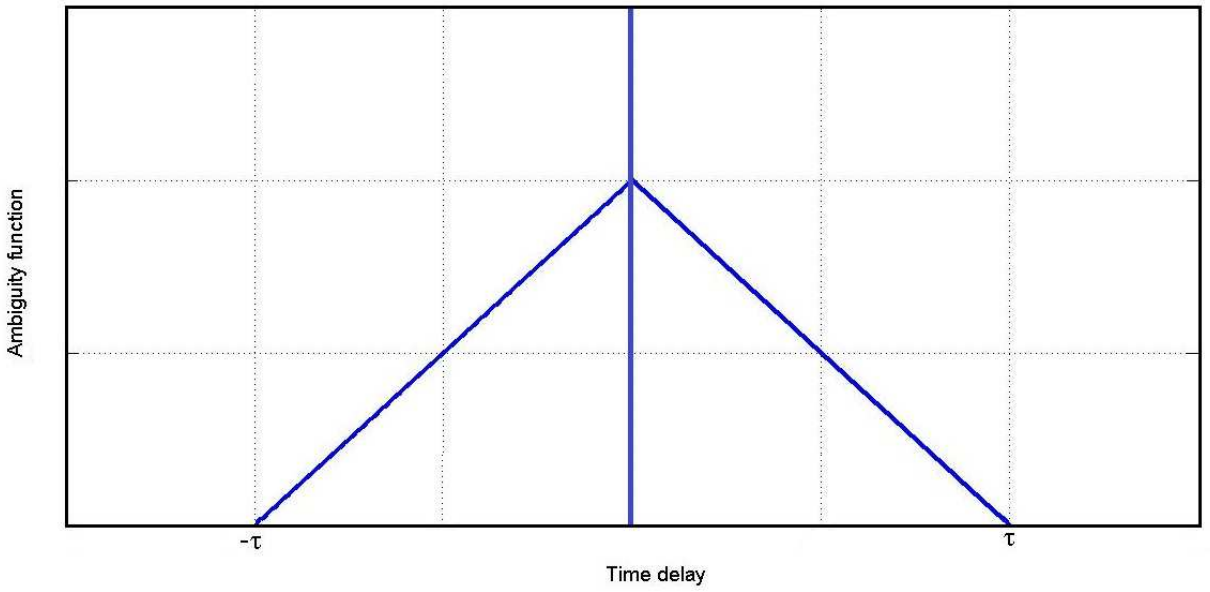

Figure 2.11: Ambiguity function plot of single pulse, constant frequency signal for zero Doppler cut.

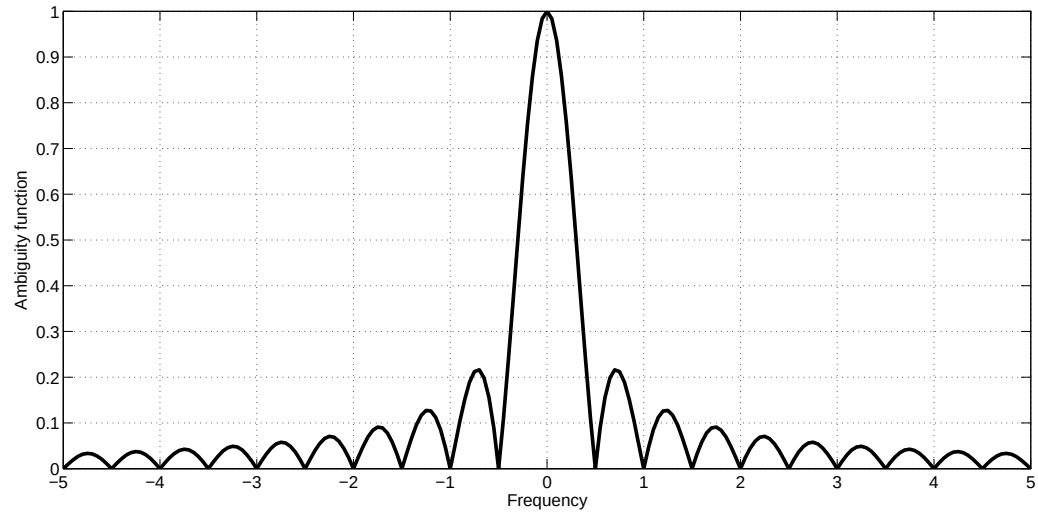

Figure 2.12: Ambiguity function plot of single pulse, constant frequency signal for zero delay cut.

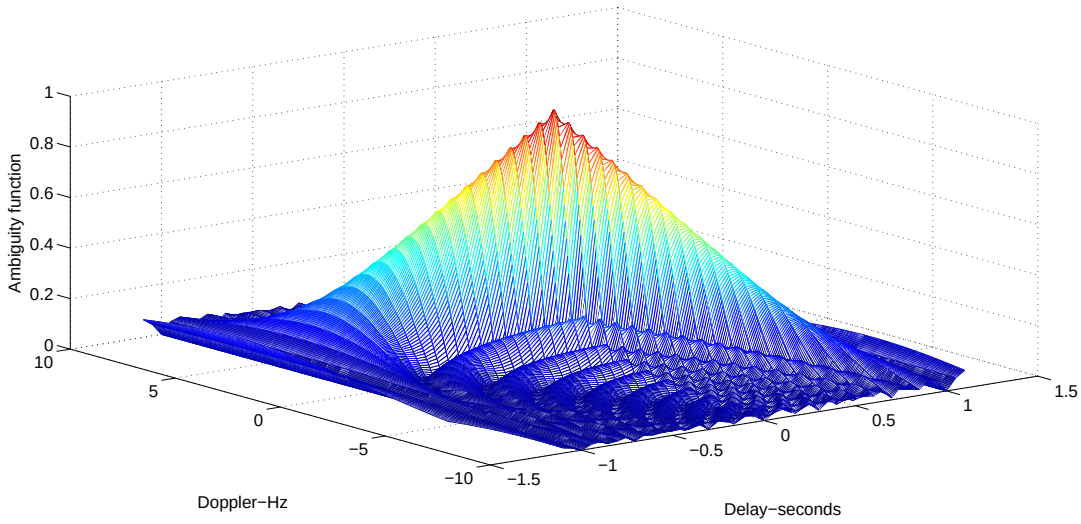

Figure 2.13: Ambiguity function plot of single LFM pulse

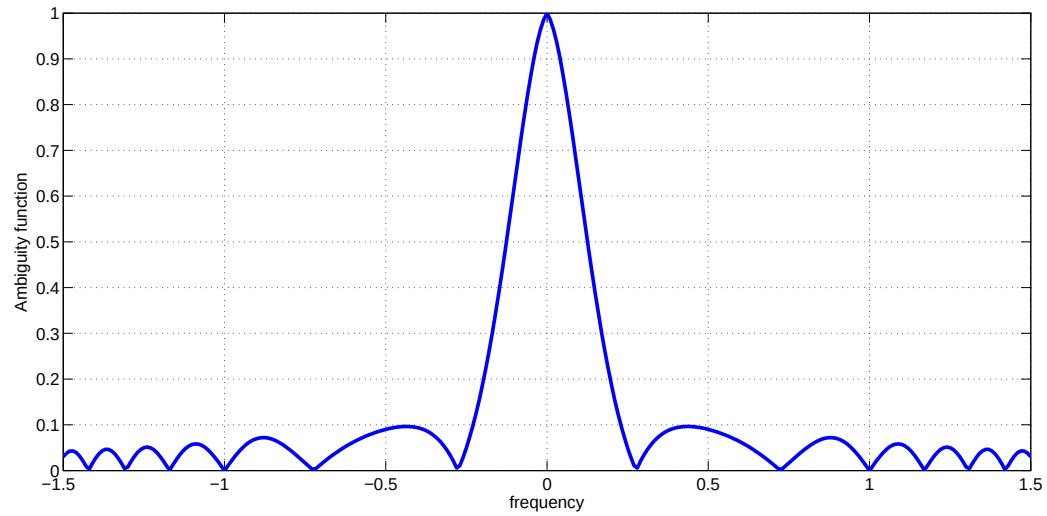

Figure 2.14: Ambiguity function plot of single LFM pulse zero Doppler cut

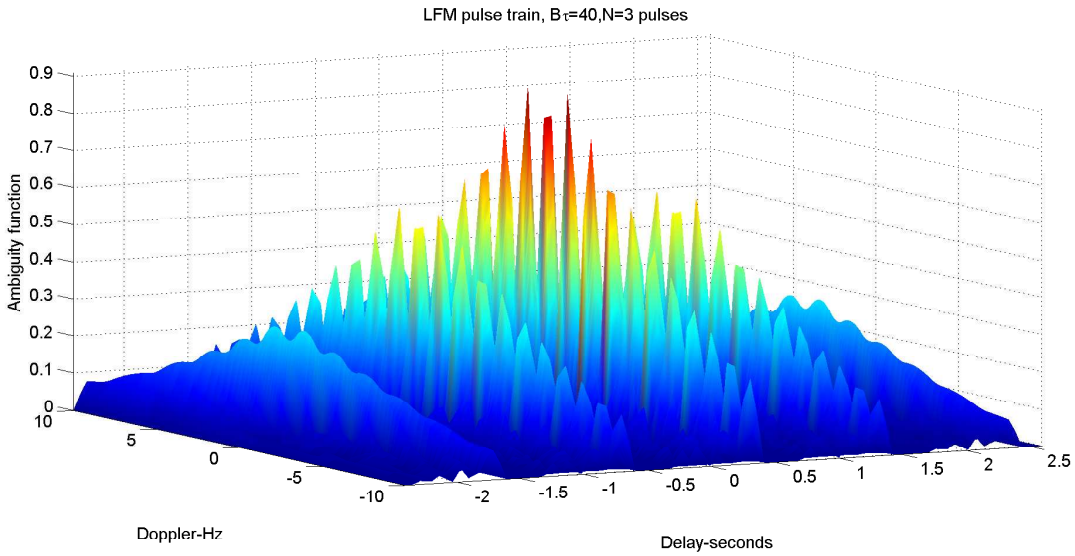

Figure 2.15: Ambiguity function plot for LFM pulse train. Number of pulse $N = 3$

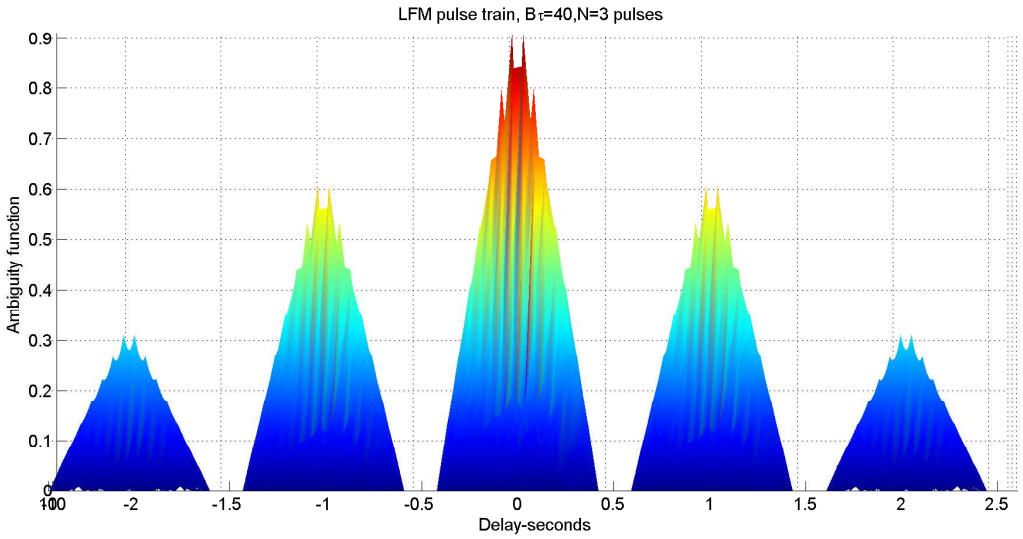

Figure 2.16: Ambiguity function plot for LFM pulse train for zero Doppler cut. Number of pulse $N = 3$

Figure 2.10 shows the ambiguity function plot of single, constant frequency pulse. In this ambiguity function no side lobes in time axis is visible. Some side lobes may be visible in Doppler axis. Figure 2.11 shows the plot of ambiguity function for zero Doppler cut. From this figure we can see that there are no side lobes present. So there is no uncertainty in detecting of the object. But the width of main lobe is very high, so the range resolution of this pulse is very poor. Figure 2.12 shows the plot of ambiguity function for zero delay cut. Here Doppler resolution is good, so we can predict the frequency shift accurately (almost accurately), but because of side lobes there will always be some uncertainty.

Figure 2.13 shows the ambiguity function plot of single LFM pulse. This figure shows the side lobes in both Doppler and Time axis. For zero Doppler cut, the ambiguity function plot is shown in Figure 2.14. For single LFM pulse, the range resolutions improves as compare to the constant frequency pulse but because of the presence of side lobe, uncertainty in finding object increases. For zero delay cut, the uncertainty increases and the resolution decreases. Figure 2.15 and 2.16 shows the plot of ambiguity function for stepped frequency pulse train and its zero delay cut. Since each waveform in SFPT is processed separately, so we get improved range resolution and less uncertainty in detecting the target.

2.7 Conclusion

This chapter presents the basic concepts of pulse compression systems. First the pulse compression and need of pulse compression is explained in this chapter, then matched filter is explained. The derivation for the matched filter response of narrow band signal is done next. To compare the performance of different radar signal, the concept of ambiguity function is explained with its property. Phase and frequency modulated signal with their advantage and disadvantage is also discussed. In last section MATLAB simulation of various radar signals is shown. In that section, we also shows and described the ambiguity function plot with their zero delay and Doppler cut. Based on the comparison of radar signal on the basis of ambiguity function we conclude that SFPT is better signal in terms of range resolution and uncertainty in object detection.

Chapter 3

Coherent Train of LFM Pulses

Introduction

Analysis of Stepped Frequency Pulse Train

Side lobe and Grating Lobe

Sidelobe Reduction

Grating lobe Reduction

Problem Formulation for Optimization

Conclusion

Chapter 3

Coherent Train of LFM Pulses

3.1 Introduction

Range resolution is one of the very important property of radar signals. The range resolution depends upon the bandwidth of the radar signal. In fact, it is inversely proportional to the bandwidth of the radar signal. If we increase the bandwidth of the signal, its range resolution will improve correspondingly. Improvement in range resolution is good for pulse compression system. Range resolution can be improved by using wide-band pulses, but bulky and costly transmitters and receivers are the drawbacks of using wide-band pulse. Also, other sources can cause interference to wide-band pulses. Another way to achieve wide-band pulse is to change linearly the center frequencies of the pulse train [8]. A fundamental waveform is used to modulate the each pulse of the pulse train. When we use LFM pulse to modulate pulse train, then the resultant signal is known as Stepped Frequency Pulse Train (SFPT) or Synthetic Wide-band Waveform (SWW). SFPT is a wide-band signal, but it can be used in the narrow-band transmitters and receivers. Using SFPT, in radar system, simplifies the design of the radar systems.

Figure 3.1 shows the frequency and amplitude plot for SFPT. Pulse train having N number of coherent pulses, duration of each pulse is T_p and repetition time is T_r. The bandwidth of each pulse is B. Δf is the frequency step between two consecutive pulses. It is assume that T_p, B and Δf remain constant throughout the pulse. Also $B > \Delta f > 0$.

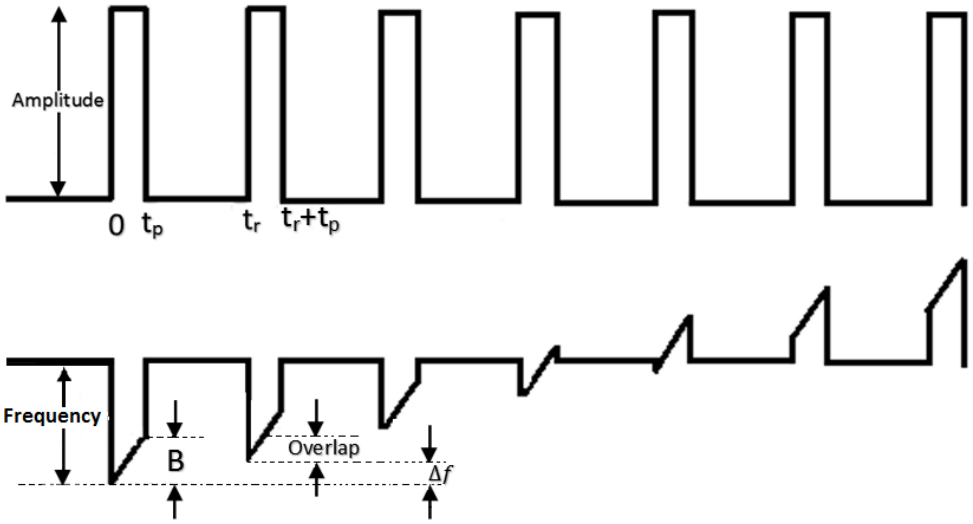

Figure 3.1: Stepped Frequency Pulse Train

3.2 Analysis of Stepped Frequency Pulse Train

The complex envelope of a unmodulated pulse (constant frequency signal) of duration T_p is given by [p. 169] [9]

$$u(t) = \frac{1}{\sqrt{T_p}} rect\left(\frac{t}{T_p}\right) \tag{3.1}$$

Frequency modulation is applied to unmodulated pulse to get an LFM Signal. The complex envelope of LFM pulse is given by

$$u_1(t) = \frac{1}{\sqrt{T_p}} rect\left(\frac{t}{T_p}\right) \exp\left(j\pi kt^2\right) \tag{3.2}$$

k is the frequency slope. k is defined in terms of the bandwidth of single LFM pulse (B) and pulse duration(T_p) as

$$k = \pm\frac{B}{T_p} \tag{3.3}$$

Here $+$ and $-$ signs are for positive and negative frequency slope respectively. In this analysis, positive value of k is used but the analysis is equally valid for the negative value of k. Instantaneous frequency of LFM signal is given by

$$f(t) = \frac{1}{2\pi}\frac{d\left(\pi kt^2\right)}{dt} \tag{3.4}$$

A uniform pulse train having N number of LFM pulses separated by $T_r \geq 2T_p$

is expressed as

$$u_N(t) = \frac{1}{\sqrt{N}} \sum_{n=0}^{N-1} u_1(t - nT_r) \tag{3.5}$$

To maintain unit energy the multiplication factor $\frac{1}{\sqrt{N}}$ is included in the expression. Further a slope of k_s is applied to entire LFM pulse train. The complex envelope of resultant signal is represented as

$$u_s(t) = u_N(t) \exp\left(j\pi k_s t^2\right)$$

$$u_s(t) = \frac{1}{\sqrt{N}} \exp\left(j\pi k_s t^2\right) \sum_{n=0}^{N-1} u_1(t - nT_r) \tag{3.6}$$

where

$$k_s = \pm \frac{\Delta f}{T_r} \qquad \Delta f > 0 \tag{3.7}$$

$+$ and $-$ signs stand for positive and negative frequency slope respectively. The overall bandwidth of SFPT is expressed as

$$B_T = (k + k_s) T_p \Delta f \tag{3.8}$$

The ACF of $u_s(t)$ is Obtained in [9] as

$$|R(\tau)| = \left| \left(1 - \frac{|\tau|}{T_p}\right) \sin c \left(B\tau \left(1 - \frac{|\tau|}{T_p}\right)\right) \right| \left| \frac{\sin(N\pi\tau\Delta f)}{N \sin(\pi\tau\Delta f)} \right| \tag{3.9}$$

The expression for $|R(\tau)|$ is product of two terms. First one is the ACF of single LFM pulse and is given by

$$|R_1(\tau)| = \left| \left(1 - \frac{|\tau|}{T_p}\right) \sin c \left(B\tau \left(1 - \frac{|\tau|}{T_p}\right)\right) \right| \tag{3.10}$$

and the second term produces grating lobe in ACF of SFPT.

$$|R_2(\tau)| = \left| \frac{\sin(N\pi\tau\Delta f)}{N \sin(\pi\tau\Delta f)} \right| \qquad \tau \leq T_p \tag{3.11}$$

3.3 Side lobe and Grating Lobe

Side lobe will result in the ambiguity function plot of signal when we try to squeeze the main lobe width. From the property of ambiguity function, if we try

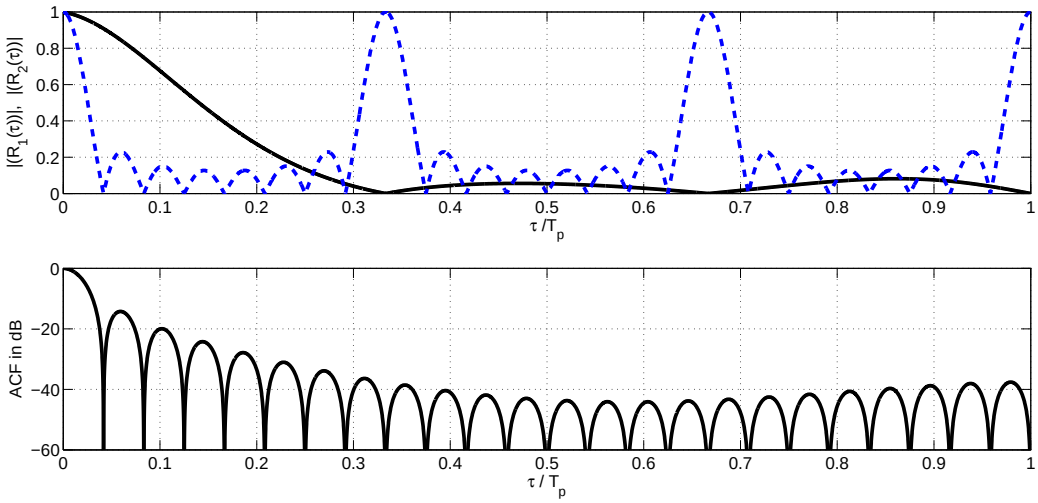

Figure 3.2: SFPT for $T_p\Delta f = 3$, $T_pB = 4.5$ and $N = 8$. Top shows $|R_1(\tau)|$ in solid line and $|R_2(\tau)|$ in dashed line. Bottom shows ACF in dB.

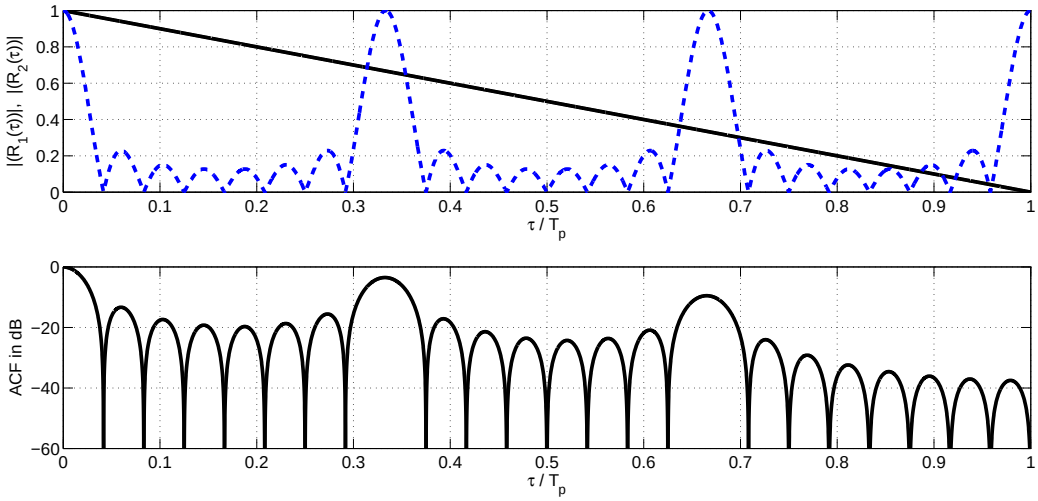

Figure 3.3: Constant frequency pulse train for $T_p\Delta f = 3$, $T_pB = 0$ and $N = 8$. Top shows $|R_1(\tau)|$ in solid line and $|R_2(\tau)|$ in dashed line. Bottom shows ACF in dB.

to reduce the main lobe width, then the volume must appear somewhere else. This volume appears near the main lobe width in the form of side lobes. The more we try to squeeze main lobe width, the more side lobes will appear.

Grating lobe is defined as the side lobe, which is having significant energy as compared to main lobe. The grating lobe are produced in ACF of radar signal because of the frequency overlap between two consecutive pulses. Grating lobe

appears when the product of pulse duration and frequency step become more than one ($T_p\Delta f > 1$).

The ACF of SFPT is given in Equation 3.9. In this equation $|R_1(\tau)|$ is the ACF of single LFM pulse. $|R_2(\tau)|$ comes because of N number of pulses used. $|R_2(\tau)|$, given by Equation 3.11, is responsible for producing the grating lobes.

Figure 3.2, 3.3 shows the plot of ACF of SFPT, for different values of $T_p\Delta f$ and T_pB. Figure 3.2 shows the plot of ACF of SFPT for $T_p\Delta f = 3$ and $T_pB = 4.5$. In this figure, we can see that $|R_2(\tau)|$ exhibits grating lobe at location $g/\Delta f$. These grating lobe have very low effect on the magnitude of ACF. The magnitude plot of $|R(\tau)|$ is also shown below. In the magnitude plot high side lobes can be seen near the main lobe. The peak side lobe level in this case is $-13.2\ dB$ below the main lobe.

Figure 3.2 shows the plot of ACF of constant frequency pulse train for $T_p\Delta f = 3$ and $T_pB = 0$. The magnitude plot of ACF shows grating lobe at location $\tau/T_p = 0.35$ and at 0.65. The magnitude plot shows high side lobes and grating lobes. The amplitude of grating lobe is considerable. These grating can be misunderstood as a second target, so they are undesirable in the plot of ACF.

3.4 Side lobe Reduction

The matched filter response of LFM signal has very high peak side lobes ($-13.2\ dB$ below the main lobe level). These high side lobes might not be acceptable in some radar applications. These high side lobes might be mistaken for a target, or they may hide a weak target. Transmitting non-uniform amplitude pulse is one way to reduced these side lobes. This can be done by applying amplitude weighting over pulse duration T_r (also known as windowing). Unfortunately, this method is not practical for high power radar. High power transmitter such as Traveling wave tubes, Klystrons should be operated saturated to obtain maximum efficiency. They can't be operated with amplitude modulation. They should be operated in either full-on or full-off. Solid state transmitter can be amplitude modulated because of linear input-output relation, provided that they are operating in

Table 3.1: Weighting function to reduce the side lobes

Weighting function	Peak side lobe (dB)	Loss (dB)	Mainlobe width (relative)
Uniform	-13.2	0	1.0
$0.33+0.66\cos^2(\pi f/B)$	-25.7	0.55	1.23
$\cos^2(\pi f/B)$	-31.7	1.76	1.65
$0.16+0.84\cos^2(\pi f/B)$	-34.0	1.0	1.4
Taylor $\overline{n}=6$	-40.0	1.2	1.4
$0.08+0.92\cos^2(\pi f/B)$	-42.8	1.34	1.5

Class-A. Solid state transmitter always operates in Class-C because of the much higher efficiency of Class-C.

Another method of reduce the side lobe is by applying amplitude weighting at the receiver end. Since the filter used for pulse compression is matched filter, using amplitude weighting results in mismatch filter. This also results in a loss of SNR. Table 3.1 gives the example of weightings, the peak side lobe, and other properties of the output waveform.

The mismatched-filter loss can be kept to about 1 dB when the peak side lobe level is reduced to 30 dB below the main lobe level. Theoretically it is possible to have no loss in SNR and still achieve low side lobes with a uniform amplitude transmitter if nonlinear LFM is used.

3.5 Grating lobe Reduction

Different methods are given in literatures for complete rejection or acceptable suppress of grating lobes. In [10,11] the pulse width is varied to reduce the grating lobes but varying pulse width destroys the periodicity of the pulse train. A method describes in [12] for grating lobe suppression. In this method energy of pulse train is distributed non-uniformly over the desired frequency band to get reduced grating lobe, higher range resolution and lower range side lobes, but spectral weighting applied for non-uniform distribution of energy, introduces additional losses in sensitivity. In [9], Levanon and Mozeson have given a relationship for $T_p\Delta f, T_pB$ and $B/\Delta f$. If the parameter of SFPT satisfy this relation then we can completely nullify the first two grating lobe. Authors have also shown that in some cases,

nullifying first two grating lobe results in nullification of all the grating lobes.

To establish such a relation between parameters of SFPT is too difficult, also in this approach N should be large if we want a significant increase in bandwidth. In [13] the grating lobes are reduced to an acceptable level by forcing the amplitude of ACF of a single frequency LFM pulse, below a predefined level at the location of grating lobe. The above mentioned approach does not reduce the range side lobe that occur near the main lobe. Non-Linear Frequency Modulated (NLFM) is used instead of LFM pulse for suppression of range side lobe but NLFM waveforms are not Doppler tolerant. A Multi-Objective Optimization (MOO) technique (Nondominated Sorting Genetic Algorithm (NSGA-II) [14]) is used by Sahoo and Panda [15] to find the parameter of SFPT for side lobes and grating lobes suppression. The complexity of the algorithm is $O(MN^2)$. M is the number of objective function used for optimization and N is the number of solution used in optimization process. In search of better Pareto front and reduced complexity, Kumar and Sahoo in [16] used Multi Objective Particle Swarm Optimization (MOPSO) [17] algorithm. This algorithm has computational complexity of $O(MN)$. This works gives the lower peak side lobe for a particular grating lobe amplitude.

3.6 Problem Formulation for Optimization

The grating lobe and side lobes affects the range resolution of SFPT and may hide weak targets. so it is required to suppress or nullify these grating lobes and range side lobes. In this work, the minimization of grating lobe and side lobe has been studied in two different way, which are as follow.

3.6.1 Problem Formulation-1

In the output of matched filter the maximum side lobe level should be low as compare to main lobe level. To minimize the side lobe level Peak to Sidelobe Ratio (PSR) is used as a objective function. PSR is defined in [15] as

$$PSR = \frac{Maximum\ sidelobe\ level\ in\ ACF}{mainlobe\ level} \tag{3.12}$$

Also for grating lobe suppression the function defined in equation 3.10 should

be minimum or zero at $\tau = \tau_g$ (grating lobe location). To have a meaningful improvement in range resolution the bandwidth of SFPT must be more than that of LFM pulse i.e. $N\Delta f > B$.

From equation 3.9, 3.10 and 3.11, we observed that ACF, $|R_1(\tau)|$ and $|R_2(\tau)|$ are function of $T_p\Delta f$ and T_pB only for a given value of N. If we choose suitable value of $T_p\Delta f$ and T_pB then grating lobe as well as side lobe can be minimized. T_pB is chosen by the following expression

$$T_pB = (c+1)T_p\Delta f \tag{3.13}$$

c is a positive number to ensure $B > \Delta f$. A positive value of c ensure that there will be some overlap in frequency of consecutive pulse. Based on the discussion above, the objective functions, for optimization, can be formulate as [15]

$Minimize\, f_1 = \max\left[\left|R_1(\tau_g)\right|\right] \quad where\, g = 1,2,\ldots\left\lfloor T_p\Delta f\right\rfloor$

$Minimize\, f_2 = PSR\ in\ dB$

$Subjected\ to\ the\ constraints\ NT_p\Delta f > T_pB$

3.6.2 Problem Formulation-2

The main lobe width depend upon the first overall null of the expression $|R_1(\tau)|$ and $|R_2(\tau)|$. The first null of $|R_2(\tau)|$ occurs at $\frac{1}{NT_p\Delta f}$ and the first null of $|R_1(\tau)|$ occurs at $\frac{1}{T_pB}$ approximately, if $T_pB >> 1$. So the location of first overall null of ACF is given by $|R_2(\tau)|$, which is equal to

$$\frac{\tau_{1st\,null}}{T_p} = \min\left(\frac{1}{T_pB}, \frac{1}{NT_p\Delta f}\right) \tag{3.14}$$

under the assumption that $T_pB >> 1$, the width of delay resolution depends on $|R_2(\tau)|$, which is equal to $\frac{1}{NT_p\Delta f}$. In literature some weighting methods available, which can be used to reduce the side lobes of an LFM pulse. By using weighting techniques, we emphasize centre frequency more as compare to end frequencies, which result in suppressed side lobe and widened main lobe. Wide main lobe decreases the range resolution. This outcome is also applicable for SFPT as we have used the condition $B > \Delta f > 0$.

In this problem we uses an objective of minimization of main lobe width. The other objective is minimization in PSR, which is same as problem-1. To ensure that grating lobes are suppressed, we add a constraint. This constraint ensure that maximum grating lobe amplitude is below a predefined level. Another constraint is added to ensure that bandwidth of SFPT is more than LFM pulse i.e. there will be some overlap in frequency. The objective functions for this problem, are as follow:

$$Minimize\, f_1 = \frac{1}{NT_p\Delta f}$$

$$Minimize\, f_2 = PSR\ in\ dB$$

$$Subjected\ to\ the\ constraints$$

$$NT_p\Delta f > T_pB$$

$$\left|R_1(\tau_g)\right| < \varepsilon$$

3.7 Conclusion

This chapter gives us the basic understanding of coherent train of LFM pulses, also known as stepped frequency pulse train. In this chapter, first we derive the expression for ACF of SFPT. From the expression of ACF side lobes and grating lobe are explained. Then the techniques available in literature to suppress side lobe and grating lobe is discussed. By combining the side lobe and grating lobe suppression techniques we formulate two problems, which can be used to suppress both side lobe and grating lobe.

Chapter 4

Multi-Objective Optimization

Introduction

Definitions

NSGA-II

IDEA

MOPSO

Performance Comparison Matrices

Performance Comparison of MOO Algorithms

Simulation Results

Conclusion

Chapter 4

Multi-Objective Optimization Techniques

4.1 Introduction

In single-objective optimization problems, we want to find the best solution of the problem which is mostly the minimum or maximum value of the objective function. In practice, the optimization problem have many objective functions. The objective functions mostly are conflicting in nature. In this type of problem, we might not have one minimum or maximum solution, which is valid for all the objective functions. In MOO problem, there exists a set of solutions that are better than the other solutions for all the objective functions, but they are equally better among themselves. such solutions are called nondominated solutions or Pareto optimal solutions. Every solution in nondomination set is an acceptable solution. With the help of extra information about the objective function, we can find dominance of one solution over the others. The MOO algorithms used are described in Section 4.3, 4.4 and 4.5. The basics concepts of MOO are described below.

4.2 Definitions

To explain the multi-objective optimization techniques, and to understand the result, some non-ambiguous definitions are required. These definitions are presented in this section.

4.2.1 Single Objective Optimization

When the optimization problem only have one objective function than optimization of such function is known as "single objective optimization". Generally in single objective optimization problem, we find the minimum value of the objective function. For optimization of maximization problem, first the problem is changed to the minimization type problem.

4.2.2 Multi-Objective Optimization

In Multi-Objective Optimization (MOO) problem, we have more than one objective function to simultaneously optimized under some constraints. In MOO problem, we search for a set of solutions (decision variable) which satisfies the constraints and gives the optimum value of objective functions. The objective functions generally conflict with each other. Hence, our aims is to find a set of solutions, which are nondominated with respect to each other, and can optimized (minimize) the objective functions. The MOO problem can be written as:

$$\begin{aligned} &Minimize \;\; f_1(x), ..., f_k(x) \\ &Subject to \;\; g_i(x) \geqslant 0, \;\; i = 1, ..., m \end{aligned} \tag{4.1}$$

4.2.3 Pareto Optimality

A solution $\vec{x}^* \in \Omega$ is said to be Pareto optimal if for every $\vec{x} \in \Omega$ and $I = \{1, 2, ...k\}$ either

$$\forall_{i \in I}(f_i(\vec{x}) = f_i(\vec{x}^*)) \tag{4.2}$$

or, there is at least one $i \in I$ such that

$$f_i(\vec{x}) > f_i(\vec{x}^*) \tag{4.3}$$

In other words, a solution is Pareto optimal, when there are no other feasible solution, in a set of solutions, which gives decrease in one objective function, without increasing one or more objective functions values.

4.2.4 Pareto Dominance

A solution $\vec{u}$ is aid to dominate $\vec{v}$, if and only if $\vec{u}$ is partial less than $\vec{v}$,i.e. $\forall i \in \{1,2,...k\}, u_i \leq v_i \wedge \exists i \in \{1,2,...k\} : u_i < v_i$.

In simple words a solution u is said to be dominate another solution v in a solution set, when the value of objective functions is equal for solution u and v and for at least one solution objective function value of u is better than v.

4.3 Nondominated Sorting Genetic Algorithm-II

Nondominated Sorting Genetic Algorithm-II (NSGA-II) is a MOO algorithm, proposed by Deb in [14]. This work is an expansion of original NSGA algorithm given in [18]. Original NSGA was criticized because of its high computational complexity $O\left(MN^3\right)$. Also, we have to specify a sharing parameter, and there was no method to preserve the elitism. NSGA-II employs a fast nondomination sorting method. The computational complexity of new approach is $O\left(MN^2\right)$, where M is the number of objective function used for optimization and N is the population size. A selection operator is also used in this algorithm. Work of selection operator is to creates a mating pool. In mating pool, we combines the child and parent populations and select the best member for the new generation (with respect to objective function and crowding distance). Elitism is ensured by combining the child population with parent population. The working of this algorithm can be divided into three parts.

A. ***Fast Nondominated Sorting Approach***

Let the population size is N. For fast nondomination sorting approach, we calculate two entities for each member of the population:

1. domination count n_p, the number of solution that dominates the solution p.
2. S_p a set of solution, that solution p dominates.

The solutions that have their domination count as zero, we place them in first nondomination front. Now for each member p of first nondomination front,

Algorithm 1 Nondominated Sorting Genetic Algorithm-II

Required: N (Population size)
Required: *gen* (Number of generation)
Initialize *Parent Population*
Evaluate objective function
Apply nondominated sorting and crowding distance assignment
for i=1:gen **do**
    Apply tournament selection
    Apply crossover and mutation to generate offspring population
    Evaluate objective function for offspring population
    Combine parent and offspring population
    Apply nondominated sorting and crowding distance assignment to combined population
    Select N feasible individuals
end for

we visit every member q of its set S_q and reduce the domination count of q by one. In doing this, if the domination count of a solution become zero, we put that solution to next domination level. Now, the above process is continued with the next domination level. We repeat this process until all This solutions are placed in a nondomination front.

The domination count n_p of a solution available in second or higher nondomination front, can maximum be $N-1$. So, a solution p will be accessed by at most $N-1$ times before its domination counts turns into zero. When the domination count of a solution become zero, we assign a nondomination level to that solution and will not access that solution any further. Since there are at most $N-1$ such solutions, the aggregate complexity is $O\left(N^2\right)$. Therefore, the general complexity of the system is$O\left(MN^2\right)$.

B. ***Diversity Preservation***

Diversity preservation is used, so that the obtain Pareto front maintain an excellent spread of the solutions. In original NSGA, we need to specify a sharing function for diversity preservation. In this algorithm sharing function approach is replaced by a crowd comparison method. In this approach, we first estimate the density, then we apply crowd comparison operator.

1. **Density Estimation:** It estimate density of solutions, surrounding about a

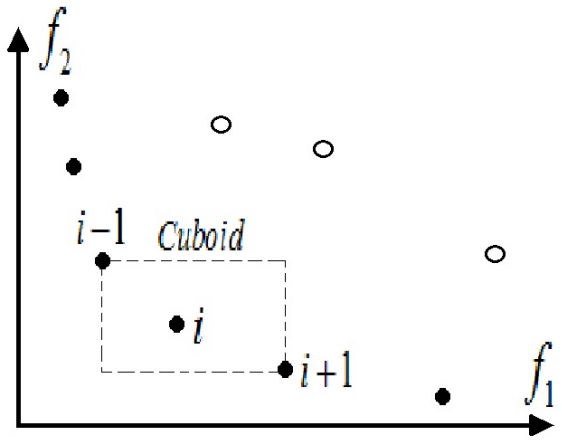

Figure 4.1: Crowding distance calculation

specific solution. We calculate the average distance ($i_{distance}$) of solutions surrounding the solution on either side of this solutions along each of the destinations. Figure 4.1 shows the solution in the front with solid circles. To calculate crowding distance for solution i, we form a cuboid between solution $i+1$ and $i-1$ (dashed box). The crowding distance for solution i is the average length of side in the cuboid.

To analyze solutions on the basis of crowding distance, we first sort the population in rising order of objective function value. The boundary solutions, for each objective functions, are assigned a distance value of infinite. To assigned distance value to Solutions in between the boundary solutions, we calculate, for two adjacent solutions, the absolute normalized difference of objective function values. For each objective function, we repeat this procedure. The sum of all the distance calculated for a solution is known as the crowding distance. Before calculating crowding distance, we first normalized the objective function value.

2. **Crowed-Comparison Operator:** The crowd comparison operator is denoted by $\prec_n$. It guides the selection process to a uniform spread-out Pareto optimal front. We assume that every solution i is having two attributes:

   a. Nondomination rank (i_{rank});

b. Crowding distance ($i_{distance}$).

we now define a partial operator $\prec_n$ as

$$\begin{aligned} & i \prec_n j \quad if\,(i_{rank} < j_{rank}) \\ & or \quad ((i_{rank} = j_{rank}) \\ & and \quad (i_{distance} > j_{distance})) \end{aligned} \tag{4.4}$$

In crowd comparison, we prefer the solution that is in lower nondomination front. If both solutions are in same nondomination front, then we chose solution whose distance metric is large means solution located in the lesser crowded area.

C. ***Main Loop***

In this algorithm, for the very first generation, we create a random population P_0 of size N. Then we apply nondomination sorting on the population and assign a rank (equal to its nondomination level) to each solution. At first, the binary tournament is chosen to select the parent for crossover and mutation operator. Simulated binary operator is used for crossover. This operation gives us child population Q_0 of size N. Now we combine the child population with parent population. Elitism is introduced in this algorithm by comparing current population with previously found best-nondominated solutions, the procedure is different after the initial generation. The t^{th} generation of this algorithm is shown in Figure 4.2.

For t^{th} generation the combined population is denoted as $R_t = P_t \cup R_t$.The size of R_t is $2N$. The population R_t is sorted based on nondomination criterion. Since all previous and current population members are included in R_t, elitism is ensured. Now, the solutions in first nondomination front F_1 are the best solutions of the total population, so we prefer the solution of first nondomination front. If the total number of solution in first nondomination front is less than N, then we choose all the solution of first front for new population p_{t+1}. The remaining members of the population p_{t+1} are chosen from subsequent nondominated fronts in the order of their ranking. Thus, solutions from the set F_2

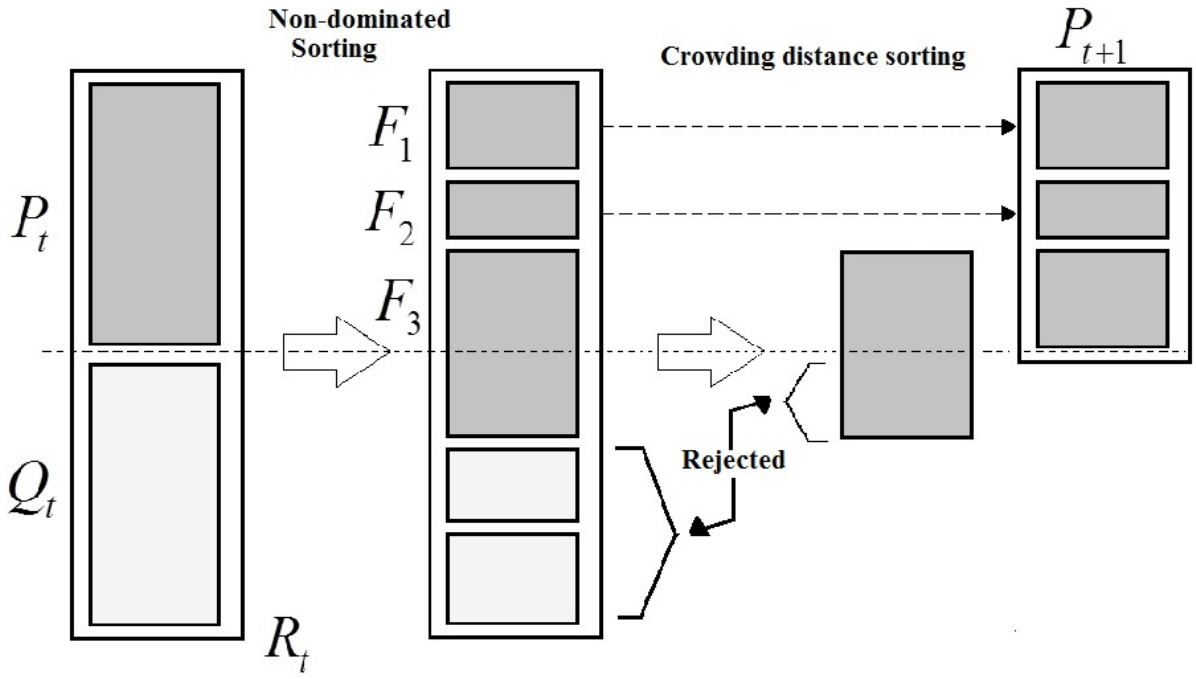

Figure 4.2: NSGA-II procedure

are chosen next, followed by solutions from the set F_3, and so on. We repeat this procedure until we are unable to accommodate the next front. Let's say that the set F_l is the last nondominated set beyond which no other set can be accommodated. The total number of solutions from F_1 to F_l is more than N. To accommodate exactly N number of solution in P_{t+1}, we choose remaining solution from F_l. we sort the solutions of the last front F_l using the crowded-comparison operator $\prec_n$ in descending order and choose the best solutions needed to fill all population slots.

The new population P_{t+1} of size N is now used for selection, crossover, and mutation to create a new child population Q_{t+1}. NSGA-II use binary tournament selection operator but the selection criterion is based on crowded-comparison operator $\prec_n$.

4.4 Infeasibility Driven Evolutionary Algorithm

The performance of multi-objective optimization algorithm depends on how we handle the constraints. The optimization algorithms available in literature choose a solution which does not violate the constraint (feasible solution) over a solution which violate the constraint (infeasible solution) during the search for optimum solution. This drives the algorithm to check the feasibility of population first before improving the objective functions. In this way, the algorithm tries to approach the constraint boundary from the feasible side. In some optimization problem, it may happen that the optimal solution lies just outside the constraint boundary. In this type of problem, typical algorithms are failed to give this optimum result.

In this algorithm, presented and explained in [19–21], we maintain a small percentage of infeasible solutions in the population at every generation, during the course of the search. By keeping some infeasible solution in the population, we try to approach a solution point where we marginally satisfy the constraint (constraint boundary). we try to approach that point from feasible side of constraints boundary as well as infeasible side of constraints boundary. The pseudo-code for this algorithm is shown in Algorithm 2. A MOO problem can be written as

$$\begin{aligned} &Minimize \;\; f_1(x), ..., f_k(x) \\ &Subject to \;\; g_i(x) \geqslant 0, \;\; i = 1, ..., m \end{aligned} \tag{4.5}$$

where $x = \{x_1, ..., x_n\}$ is the decision variable. Each decision variable is bounded by the lower and upper boundary. In IDEA algorithm, we change original k objective MOO problem to $k+1$ objective problem. The modified problem can be written as:

$$\begin{aligned} Minimize \;\; f'_1(x) = f_1(x), ..., f'_k(x) = f_k(x) \\ f'_{k+1}(x) = Violation measure \end{aligned} \tag{4.6}$$

The first k objective remain same as given in Equation 4.5. The $k + 1^{th}$ objective is known as violation measure, calculate by using constraints. The steps of this algorithm are outlined in Algorithm 2. Like NSGA-II, IDEA also uses binary tournament selection for selection of two random parent, simulated binary crossover

Algorithm 2 Infeasibility Driven Evolutionary Algorithm

Required: N (Population size)
Required: gen (Number of generation)
Required: $0 < \alpha < 1$ (Proportion of infeasible solutions)
$N_{\text{inf}} = \alpha * N$
$N_f = N - N_{\text{inf}}$
Initialize $POP()$
Evaluate $POP()$
for i=2:gen **do**
  $childpop_{i-1} = Evolve(pop_{i-1})$
  Evaluate $childpop_{i-1}$
  $\left(S_f, S_{\text{inf}}\right) = Split\left(pop_{i-1} + childpop_{i-1}\right)$
  Rank (S_f)
  Rank (S_{inf})
  $pop_i = S_{\text{inf}}\left(1, N_{\text{inf}}\right) + S_f\left(1, N_f\right)$
end for

(SBX), mutation for the evolution of child population from parent selected. The difference between IDEA and the NSGA-II is the procedure for preservation of elite population. For elite preservation in NSGA-II, we combined the feasible child and feasible parent population and then select new population member from the combined population. In this algorithm, we maintain a small percentage of infeasible solution. While combining feasible child and feasible parent population, we also keep some infeasible population for elite preservation.

In this algorithm, every solution is evaluated as per the problem defined in Equation 4.5.If any of the constraints is violated, then that solution is marked infeasible. After evolving child population from the parent population, we combined both the population. On the basis of constraint violation measure the combined population is splitted into an infeasible set (S_{inf})and a feasible set (S_f). Now non-dominated sorting and crowding distance sorting is applied on feasible and the infeasible sets for $k+1$ objectives. NSGA-II uses non-dominated sorting to find the nondominated solutions and crowding distance for the ranking of feasible non-dominated solutions. Infeasible nondominated solutions are ranked on the basis of maximum constraint violation.

A parameter α is used in this algorithm to find the number of the infeasible

solutions. The value of parameter α is set by the user. At every generation $N_{inf}(= \alpha * N)$ number of infeasible solutions are maintained for next generation, where N is population size. If infeasible set S_{inf} has solutions more than N_{inf}, then we consider only first N_{inf} solution in infeasible set and discard the other solutions. If solutions in infeasible set are less than N_{inf}, all the solutions will be selected to infeasible set. Remaining solutions in infeasibility set will be selected from feasible set.

If feasible set has less solution than N_f, then all the solutions are get selected, and remaining solutions will be picked from infeasible set. If feasible set has more solution than N_f, then first N_f solutions will be selected from feasible set. All the solutions are marked from 1 to N, in the order they are selected. Since infeasible solutions are selected first, so they will get better rank than feasible solutions.

4.4.1 Constraint Violation Measure

The $k+1^{th}$ objective function in this algorithm is constraint violation measure. The constraint violation measure for a particular solution is based on constraint violations of individual constraints. To calculate constraint violation measure, we evaluate all the constraint. For i_{th} constraint, we sort it in ascending order based on constraint violation and assign a rank to each solution. The solution which is least violating the constraint, assigned a rank one. Next least violating solution gets the rank two. Solution with the same level of violation gets the same rank. The solution, which do not violate the constraint gets the rank zero. This procedure is repeated for all the constraints. When a solution gets a rank for each constraint, we add its rank for each constraint. The sum of ranks is known as the constraint violation measure.

The process of calculating constraint violation measure is illustrated in Table 4.1. A sample population of 10 solution is taken in this example. Let there are 3 constraint for our problem. For each solution constraint violations is shown in first three columns. For each constraint, we sort the constraint violation in ascending order for combined population. Each solution will get relative ranks, shown in

Table 4.1: Calculation of constraint violation measure

Solutions	Violations			Relative ranks			Violation measure
	C1	C2	C3	C1	C2	C3	
1	70.60	105.61	36.71	8	9	3	20
2	8.23	15.20	70.60	4	6	8	18
3	16.15	1.11	0.00	6	1	0	7
4	3.00	15.16	13.10	2	5	2	9
5	1.69	10.13	69.10	1	4	7	12
6	7.89	100.10	61.72	3	8	6	17
7	0.00	2.15	0.00	0	2	0	2
8	190.10	200.18	51.21	9	10	5	24
9	21.38	17.21	38.21	7	7	4	18
10	10.90	6.70	0.10	5	3	1	9

next three columns, for each constraint. Solution 7 does not violate the constraint for C1, Solution 3 and does not violate the constraint for C3. So we assign them rank zero. Constraint violation measure for a particular solution is the sum of relative ranks; it gets for each constraint.

With the help of constraints violation measure, we choose the solution with less violation measure. We prefer the solution that is having good rank for most (or all) of the constraints. But if a solution has significant large rank for just one solution, then the chance of selection of that solution would be same as other solution that is having marginal violations of many constraints. By doing this, we include the sum of constraint violated by the solution. IDEA uses constraint violation measure as the extra objective. We apply non-dominated sorting and rank the infeasible solutions for the added objective of constraint violation measure. As a result, the final population consists of the solutions with minimal constraint violations. The working of this algorithm can be written as:

1. Initialized population(*pop*) randomly in the given search space.
2. Evaluate objective functions and constraints.
3. Evolve child pop using NSGA-II algorithm.
4. Evaluate constraints and objective functions for child pop.

5. Combine pop and child pop.
6. For any solution i, if any constraint is violated then put that solution in infeasible set, else put in feasible set.
7. Apply nondominated sorting and crowding distance assignment to feasible set.
8. Apply nondominated sorting and crowding distance assignment to infeasible set.
9. Take first N_{inf} solution from infeasible set and N_f solution from feasible set to form new pop.
10. Repete steps 3 to 8 until *gen* is not reached

4.5 Multi-Objective Particle Swarm Optimization

James Kennedy and Russell C. Eberhart [22] initially put forward the idea of using Particle Swarm algorithm for the optimization problem. PSO model the movement of a flock of birds when they are searching for food. The original PSO algorithm is applicable for single object optimization only. In [23] Coello Coello proposed the PSO for multiple objective but coello does not provide any method for constraint handling. In [17] Coello Coello proposed an improved version of multi-objective PSO. In the improved version of MOPSO, the author have added an improved constraint handling mechanism. They have also proposed a mutation operator that enhances the exploratory capabilities of the algorithm. The secondary population found, is used by the particles to guide their flight direction. PSO has highs speed of convergence. This is the reason, why PSO is preferred in the optimization problem.

4.5.1 Algorithm Description

The algorithm is shown in Algorithm 3. The description of algorithm can be divided into four parts. First parts gives the steps involved in the algorithm. Sec-

ond part explains about the secondary population (Repository). Third part is about mutation operator used in this algorithm. Last part is about constraint handling procedure. The description of main algorithm is given below.

A. **Main Algorithm**

1. Initialized population (*pop*) randomly in the given search space and velocity (*Vel*) to zero.
2. The objective functions which are to be optimized are evaluated for each particle of population.
3. Apply nondomination sorting on population and store the positions of the nondominated particles in population to the repository *REP*.
4. Generate hypercubes of the search space visited. Coordinates of hypercubes are the objective functions value. Place all the particles in the hypercubes. Coordinates of particles are their objective functions value.
5. The memory of each particle is initialize to their personal best of first generation.
$$Pbest = pop$$
6. For each particle Compute the speed using the equation:
$$Vel(i) = w * Vel(i) + R_1 * c_1(Pbest(i) - pop(i)) + R_2 * c_2(REP(h) - pop(i))$$
where w is the inertia weight; c_1, c_2 are global and local learning coefficients respectively. R_1, R_2 are random values in the range $[0....1]$; *Pbest* is the personal best position of the particle attain up to this *gen*; $REP(h)$ is a value that is taken from the repository; $pop(i)$ is the current value of the particle i value of the particle.
7. Calculate the new value of the particle by using the expression:
$$pop(i) = pop(i) + Vel(i)$$
8. If the particles go beyond the search space, take the negative of velocity and recompute the new position using expression in previous point.

Algorithm 3 Multi Objective Particle Swarm Optimization Algorithm

Required: N (Population size)
Required: *gen* (Number of generation)
Initialize *pop()*
Initialize *Vel()*
Evaluate each particle in *pop()*
Store nondominated vectors in the *REP*
Generate hypercube
Pbest=pop
j=0
while j<gen **do**
  for each particle i **do**
    $Vel(i) = w * Vel(i) + R_1 * (Pbest(i) - pop(i)) + R_2 * (REP(h) - pop(i))$
    $pop(i) = pop(i) + Vel(i)$
    Maintain *pop(i)* within search space
    Evaluate particle i
    Update *REP*
    Update *Pbest(i)*
  end for
  $j = j + 1$
end while

9. Evaluate each of the particles in pop
10. Update the contents of REP
11. Update $Pbest$
12. Repeat steps A6 to A11 until *gen* is not reached

B. **External Repository**

The External repository stored the nondominated solution found at each generation. The external repository has two component: the archive controller and the adaptive grid.These two parts are described below:

(a) **The Archive Controller:** The archive controller decide whether a particular solution stays in the archive or not. The procedure to decide this is as follow: At the start of the search, the external repository will be empty. For the very first time, the first solution is allowed to enter the archive (case 1, in Figure 4.3). After first entry in archive controller, all

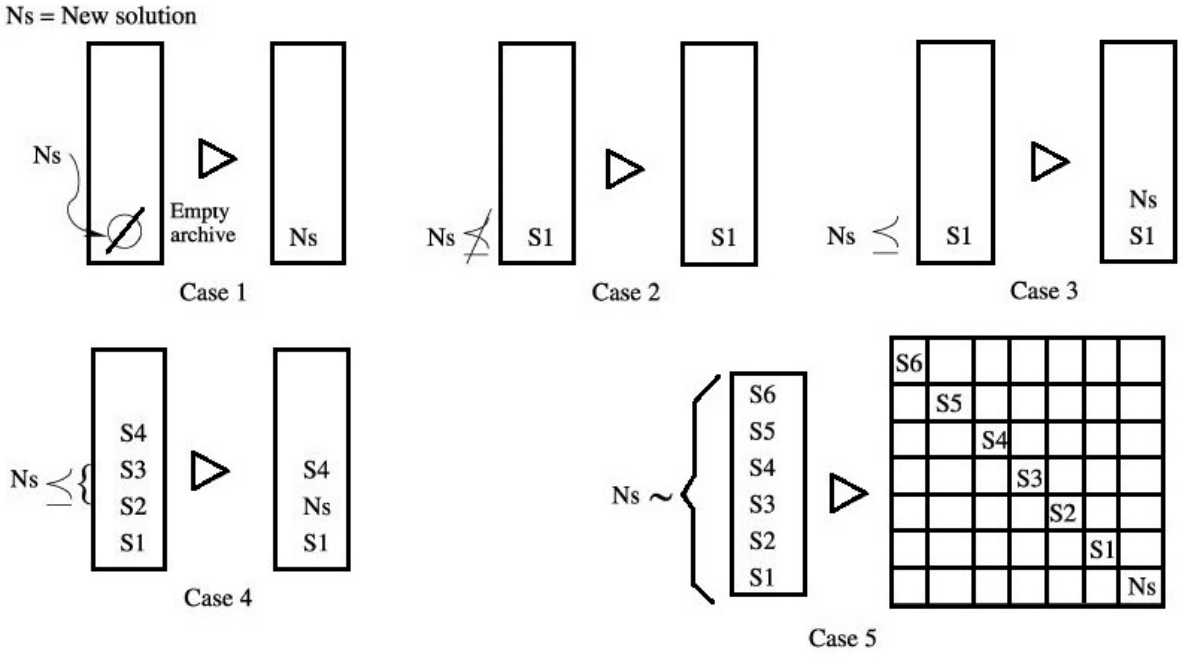

Figure 4.3: Possible cases for the archive controller

other nondominated solutions are compared (one-on-one basis) with the solutions in the external repository. If a new solution, who wants to enter the archive controller, is dominated by an individual solution within the external archive, then new solution will be rejected by the controller(case 2 Figure 4.3). In this new solution is not dominated by any other solution present in the external repository, then it will be allow to enter in the repository (case 3 Figure 4.3). If there are one or more than one solution in the repository, which are dominated by the new solution, then all the dominated solution will be deleted by the repository and new solution will allow to enter the repository(case 4 Figure 4.3). When the external repository reaches its maximum length, then it will converted into a grid and adaptive grid procedure is invoked (see case 5, Figure 4.3).

(b) **The Grid:** The Adaptive grid is used to produce the well spread Pareto front. The Adaptive grid was originally proposed in [24]. The external archive is used to store the solutions which are nondominated.

The Adaptive grid is used to produce the well spread Pareto front. The

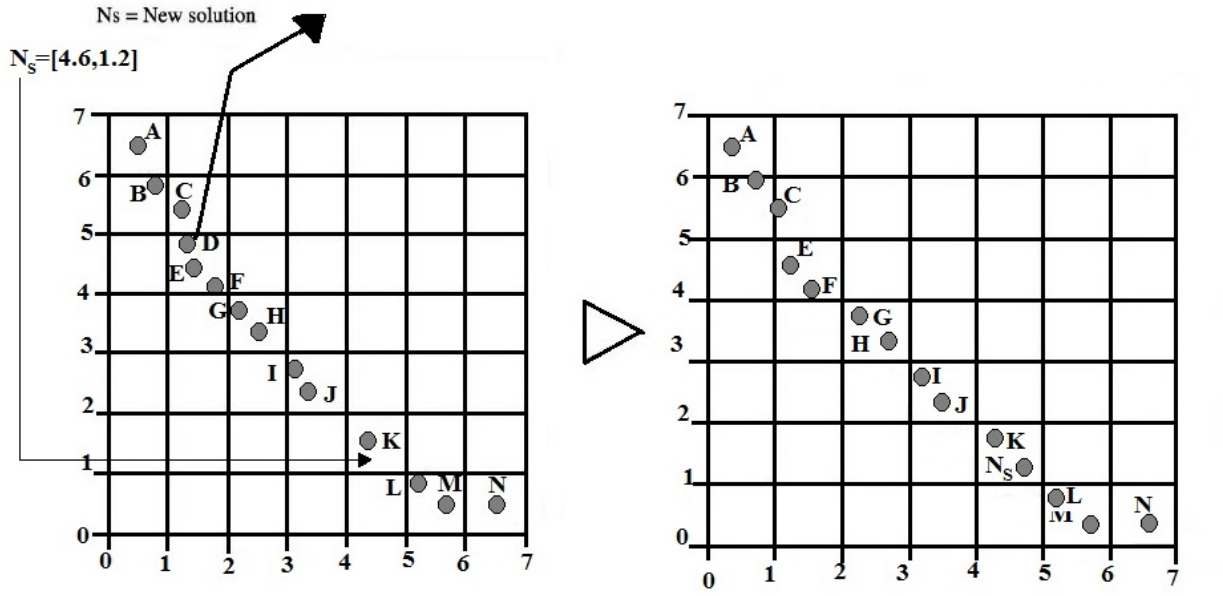

Figure 4.4: Insertion of a new solution (lies inside the boundary) in Adaptive grid.

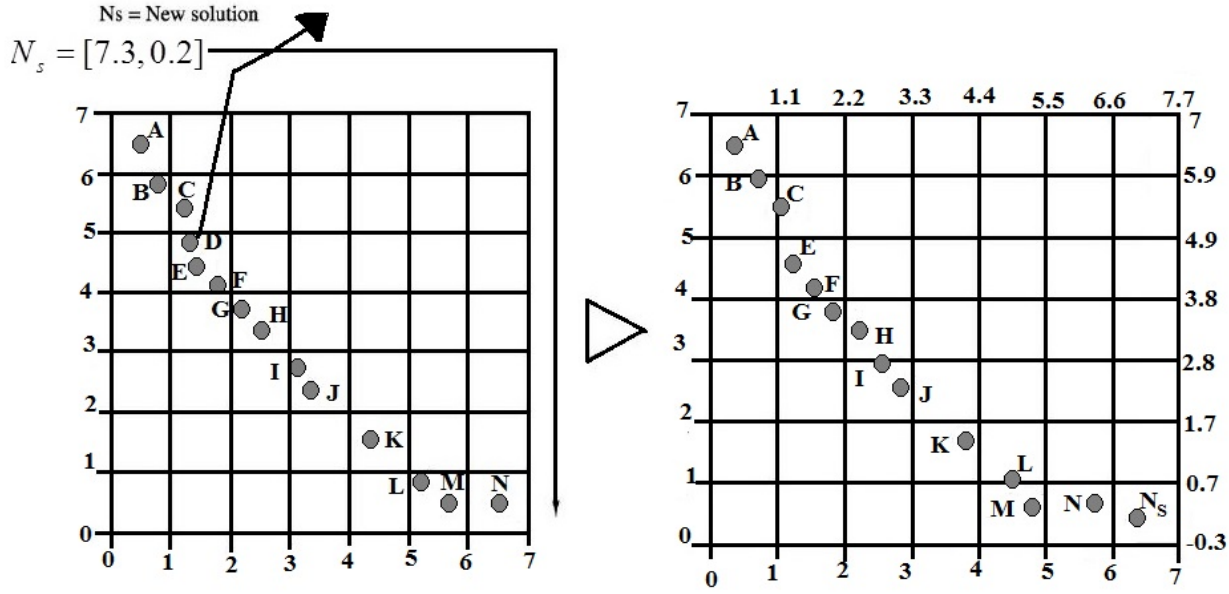

Figure 4.5: Insertion of a new solution (lies outside the boundary) in Adaptive grid.

Adaptive grid was originally proposed in [24]. The external archive, discussed earlier, stores the nondominated solutions. when external archive, reaches its maximum length , the adaptive grid procedure in evoked.

If a new solution, whose coordinates are within the grid boundary wants to enter into the repository, then we place that solution within the grid

(at its coordinate location). Placing a new solution in the grid, increase the length of the grid. (Figure 4.3).If grid reaches its maximum length; then we delete a solution from more populated area. This is equivalent to minimizing crowding distance.

If a new individual solution, who wants to enter the archive, whose coordinates are outside the current boundary of the grid. To place this solution in the grid, we have to recalculate the grid boundaries. After recalculation of boundaries, all the nondominated solution will be placed at their new location. Again if grid reaches its maximum length, then we delete a solution from more populated area. (Figure 4.4).

C. **Mutation operator**

The reason for using PSO in multi-objective is its very high conversion speed. The high speed of conversion may be harmful, because a PSO based algorithm may trap somewhere. Which will result in false Pareto front. Because of this problem, we have use a mutation operator. At the start of generation , all the particle will undergo the mutation. As the number of iteration increases, the number of particles that go through mutation operator decrease rapidly.

In this algorithm, apart from applying mutation operator to the swarm, we also use mutation to the range of the decision variable. At starting of the search, all the variable and search space go through the mutation operator. As the number of iteration increase, the number of particle and range decreases rapidly using a nonlinear function. This aims to provide a highly exploitative behavior in the algorithm.

D. **Constraints Handling**

This algorithm has very simple scheme to handle constraints. Whenever two individuals are compared, we check their constraints. If both are feasible, non-dominance is directly applied to decide who is the winner. If one is feasible and the other is infeasible, the feasible dominates. If both are infeasible, then the one with the lowest amount of constraint violation dominates the other.

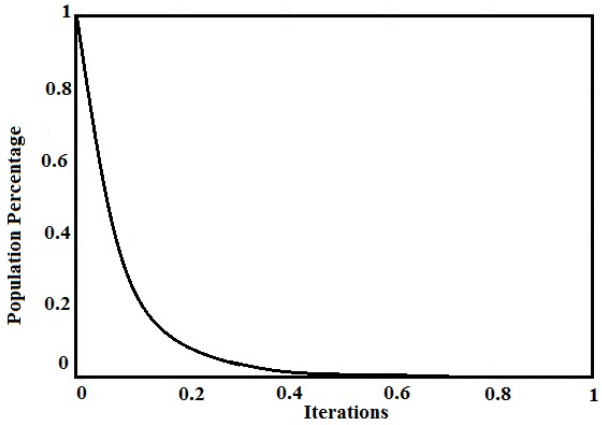

Figure 4.6: Behavior of mutation operator

4.6 Performance Comparison Matrices

In this work we use 2 performance matrices to compare the performance of the Pareto front obtained by using various MOO algorithm. These matrices are described below:

4.6.1 Convergence Matrix

Hypervolume is used to measure the convergence of a Pareto front. Hypervolume was proposed in [25, 26], by Zitzler et al. as:

$$HV\left(S,R\right) = volume\left(\bigcup_{i=1}^{|S|} v_i\right) \tag{4.7}$$

This metrics gives the volume (in the objective space) that is dominated by the optimal solution set S [27]. For example, in Fig. 4.7, $S = A,B,C$ is attained when minimizing a bi-objective Multi-Objective Problem (MOP). The HV(S,R) is the area *ABCWA* enclosed by the discontinuous boundary, where reference set $R = \{W\}^2$.

4.6.2 Diversity Matrix

Diversity matrix is used to indicate the distribution and spread of solutions in the optimal solution set S. To measure diversity, a matrix Δ' was proposed by Deb. in [28]. Δ' compares all the solutions consecutive distances with the average

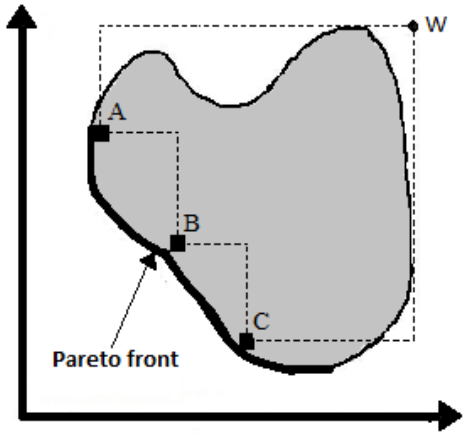

Figure 4.7: The performance metric Hypervolume (HV) in MOO.

distance:

$$\Delta'(S) = \sum_{i=1}^{|S|-1} \frac{(d_i - \overline{d})}{|S|-1} \tag{4.8}$$

Here d_i is calculate for solution set S. It is Euclidean distance between two consecutive solutions. $\overline{d}$ is the average of d_i. If all the pair of consecutive solutions share equal distance, then $d_i = \overline{d}$, $\Delta'(S) = 0$ and S has a perfect distribution. To find consecutive solutions, the prerequisite of this metric is to sort the solutions of S by lexicography order.

4.7 Performance Comparison of MOO Algorithms

In this section, performance of optimization algorithm is studied. Some single objective and multi-objective test problems are optimized using the MOO algorithms explained in this chapter. The problem and obtained result is explained below:

4.7.1 Single Objective Test Problem

To test the performance of optimizations algorithms on single objective functions, we use "G series" test problem, given in [29]. We use "G-1" and "G-6" problem given in this work. The problems are explain below:

1. **G-1 Problem**

$$\begin{aligned} &Minimize \\ &G_1(x) = 5x_1 + 5x_2 + 5x_3 + 5x_4 - 5\sum_{i=1}^{4} x_i^2 - \sum_{i=5}^{13} x_i \end{aligned} \tag{4.9}$$

Subjected to the following constraints:

$$\begin{aligned} &2x_1 + 2x_2 + x_{10} + x_{11} \leq 10, \\ &-8x_1 + x_{10} \leq 0, \\ &-2x_4 - x_5 + x_{10} \leq 0, \\ &2x_1 + 2x_3 + x_{10} + x_{12} \leq 10, \\ &-8x_2 + x_{11} \leq 0, \\ &-2x_6 - x_7 + x_{11} \leq 0, \\ &2x_2 + 2x_3 + x_{11} + x_{12} \leq 10, \\ &-8x_3 + x_{12} \leq 0, \\ &-2x_8 - x_9 + x_{12} \leq 0 \end{aligned}$$

The decision variables range for this problem are:
$0 \leq x_i \leq 1,\ i = 1,...9,\ 0 \leq x_i \leq 1,\ i = 10,11,12$ and $0 \leq x_{13} \leq 1$. This function is having 13 decision variables and 9 linear constraints.

2. **G-6 Problem**

$$\begin{aligned} &Minimize \\ &G_6(x) = (x_1 - 10)^3 + (x_2 - 20)^3 \end{aligned} \tag{4.10}$$

Subjected to the following constraints:

$$\begin{aligned} &(x_1 - 5)^2 + (x_2 - 5)^2 - 100 \geq 0, \\ &-(x_1 - 6)^2 - (x_2 - 5)^2 + 82.81 \geq 0. \end{aligned}$$

This problem have 2 decision variables and 2 constraints. The decision variables range for this problem are:

$$13 \leq x_1 \leq 100 \ \textit{and} \ 0 \leq x_2 \leq 100$$

4.7.2 Multi-Objective Test Problem

To compare the performance of MOO algorithms on multi-objective problem, we use "CTP" series test problem. "CTP" series problem was proposed by Deb

in [30]. To compare the performance we used "CTP-2" Problem. This problem is described as:

1. **CTP-2 Problem**

$$\begin{aligned} &Minimize \quad f_1(x) = x_1 \\ &Minimize \quad f_2(x) = c(x)\left(1 - \sqrt{\frac{f_1(x)}{c(x)}}\right) \end{aligned} \tag{4.11}$$

where

$$c(x) = \sum_{i=1}^{10}\left(x_i^2 - 10\cos(2\pi x_i) + 10\right)$$

Subjected to the constraint

$$\cos(\theta)(f_2(x) - e) - \sin(\theta) f_1(x) \geq a\left|\sin\left(b\pi(\sin(\theta)(f_2(x) - e) + \cos(\theta) f_1(x))^c\right)\right|^d$$

This problem has 10 decision variables. The range of decision variables x_i is $0 \leq x_i \leq 1$. The variable range depends on the chosen $c(x)$ function. The problem has six parameters $(\theta, a, b, c, d \text{ and } e)$. The value of these six parameter also depends on chosen $c(x)$ function.

4.8 Simulation Result

MATLAB simulations are carried out to compare the performance of multi-objective optimization algorithm. For each optimization process, the population size is chosen as 100. The number of generation is also taken as 100. NSGA-II and IDEA uses crossover and mutation, in the process of evolution for next generation. The crossover probability is taken as 0.9. The mutation probability is taken as 0.1. For MOPSO both global learning and local learning coefficient are chosen to 1.5. The maximum length of repository is selected as 100. The ratio of infeasible population in IDEA is 0.2. The other parameters for IDEA remain same as NSGA-II algorithm.

Figure 4.8 and 4.9 shows the simulation result for "G-1" and "G-6" test problem. The best result in literature for objective function value in "G-1" problem is -15. This result is obtained using extensive mathematical calculations. Figure 4.8 shows the plot of number of generation vs objective function value obtained at each generation for "G-1" problem. In objective function values obtained after

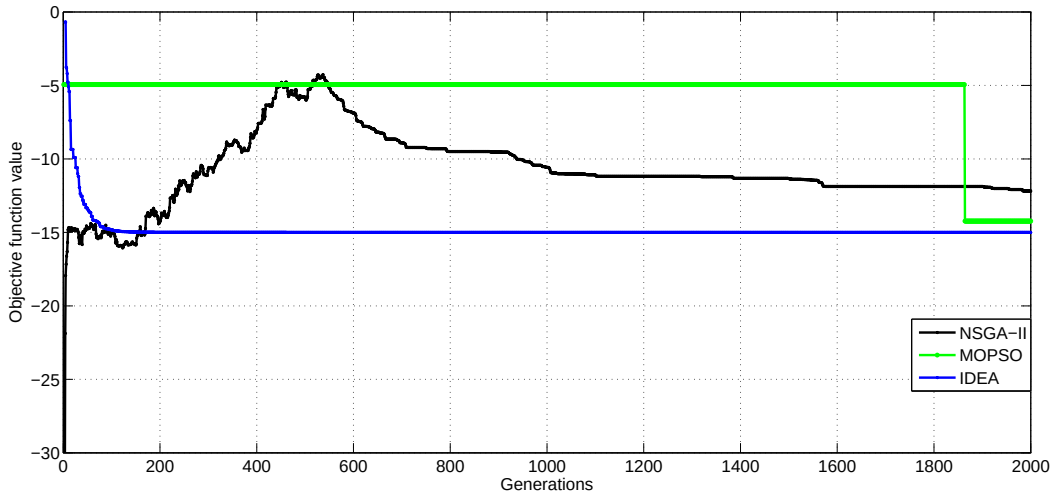

Figure 4.8: Number of generation vs objective function value for G-1 problem

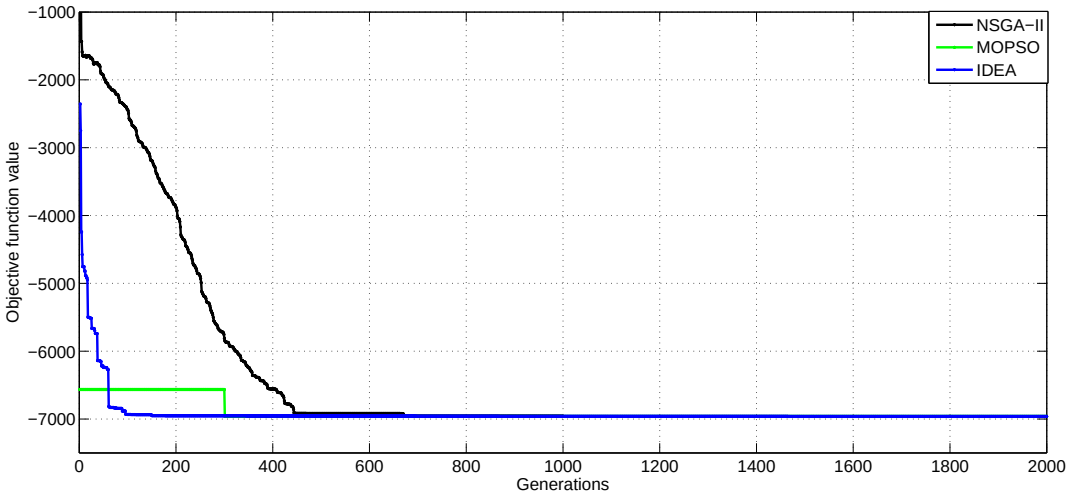

Figure 4.9: Number of generation vs objective function value for G-6 problem

2000 generations are $-12.5, -14.25$ and -15 for NSGA-II, MOPSO and IDEA algorithm respectively. From the result it is evident that IDEA is able to give us the best result. From the figure we can see that MOPSO is struck at the objective function value of -5 for almost 1900 generations. Up-to 1900 generations repository of MOPSO algorithms is have only one solutions, means MOPSO is failed to find other nondominated solutions. After 1900 generations as MOPSO algorithm finds the other nondominated solutions, it quickly converge to objective function

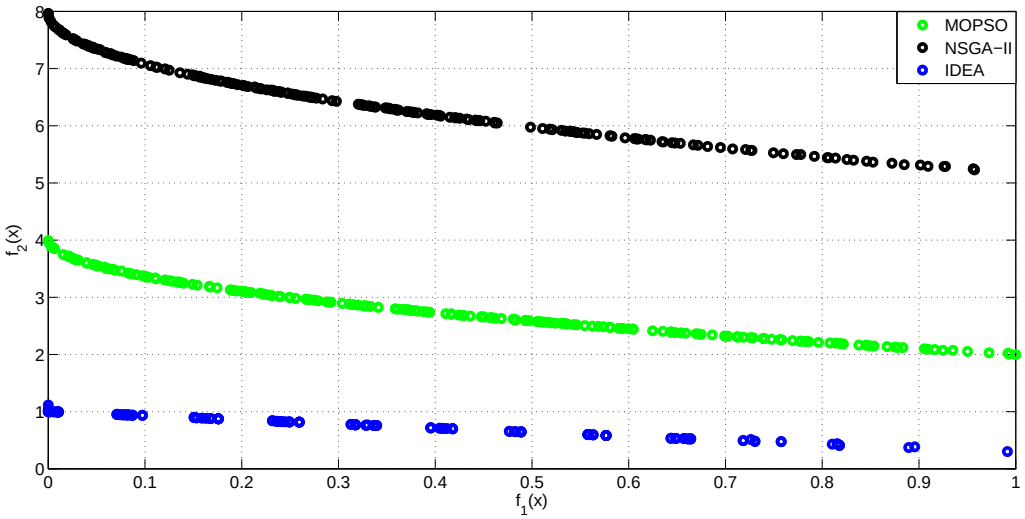

Figure 4.10: Pareto front obtained for CTP-2 problem

value of -14.25. Although the value obtained is not correct but it is close to true result. For "G-1" problem, the result obtained by IDEA algorithm is equal to best available result in literature. Also the convergence of IDEA is faster than NSGA-II and MOPSO, so we can say that IDEA is better for this problem.

Figure 4.9 shows the simulation result for "G-6" test problem. The best result in literature for objective function value in "G-6" problem is -6961.81381. For this problem, all algorithms converge to a near true value. The convergence of IDEA is faster than the others. For this problem also, MOPSO algorithm struck to a solution and after 300 iteration it can manage to obtain the true solution of the problem.

Figure 4.10 shows the Pareto front obtained for "CTP-2" test problem. For "CTP-2" problem, the best nondominated solutions lies on the constraint boundary. For this problem only IDEA algorithm is able to find solutions which are nondominated and lies on the constraint boundary. The solutions obtained by NSGA-II and MOPSO is dominated by solutions obtained by IDEA algorithm. So we can say that IDEA algorithm is better than NSGA-II and MOPSO for this test problem.

4.9 Conclusion

This chapter gives us the understanding of multi-objective optimization algorithms, their working and compare their performance. This chapter presents the basics terms used in optimization, NSGA-II, MOPSO and IDEA algorithm. The performance of these algorithm is compared for single objective and multi-objective problem. Based on the simulation results obtained, we can conclude that IDEA algorithm is better than the other two algorithm.

Chapter 5

Simulation Results

Simulation Results for Problem-1

Simulation Results for Problem-2

Conclusion

Chapter 5

Simulation Results

Simulations are carried out to find the optimized parameter of SFPT using MOO algorithms explained in Chapter 4. For each optimization process, the population size is chosen as 100. The number of generation is taken as 100. NSGA-II and IDEA uses crossover and mutation, in the process of evolution for next generation. The crossover probability is taken as 0.9. The mutation probability is taken as 0.1. For MOPSO both global learning and local learning coefficient are chosen to 1.5. The maximum length of repository is selected as 100. The ratio of infeasible population in IDEA is 0.2. The other parameters for IDEA remain same as NSGA-II algorithm. Simulation results for problem-1 and problem-1 are discussed below.

5.1 Simulation Results for Problem-1

The Pareto front obtained using NSGA-II, MOPSO and IDEA, for problem-1 is shown in Figure 5.1, 5.2. Figure 5.1 shows the Pareto front obtain for $T_p\Delta f = [2,10]$ and $c = [2,10]$. By seeing this figure, we can say that MOPSO and IDEA are giving better result than NSGA-II algorithm and the Pareto front obtained by MOPSO and IDEA is almost same. For complete suppression of grating lobe, the maximum amplitude of side lobe is given by NSGA-II algorithm is -30.8 dB below the main lobe level. While MOPSO and IDEA gives maximum side lobe -32 dB below the main lobe level. In this case there is an improvement of 1.2 dB in maximum amplitude of side lobe. For maximum grating lobe amplitude to be not more than -40 dB below the main lobe level (maximum amplitude of grating lobe to below 0.01), NSGA-II gives peak side lobe amplitude to -31.8 dB

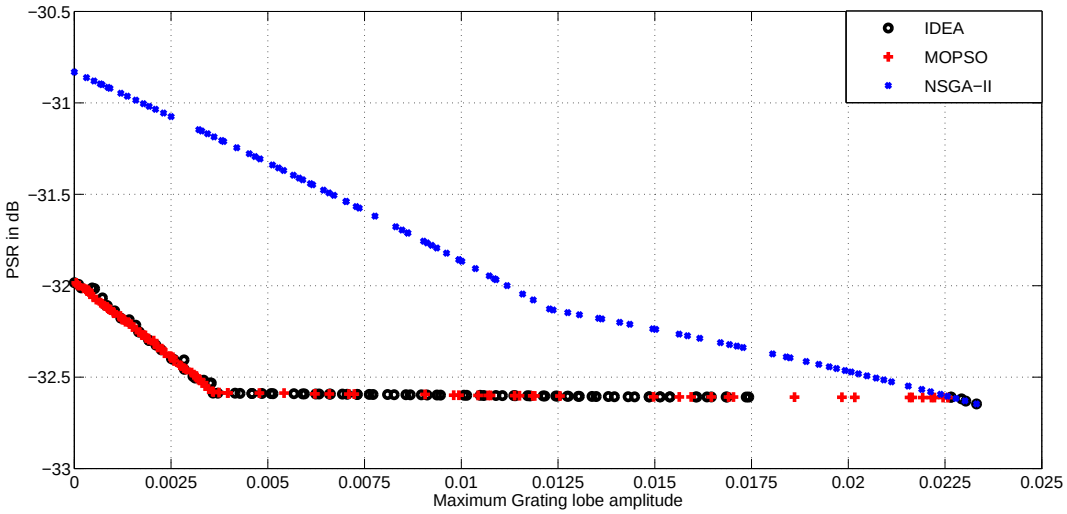

Figure 5.1: Pareto front obtained for $T_p\Delta f = [2, 10]$ and $c = [2, 10]$

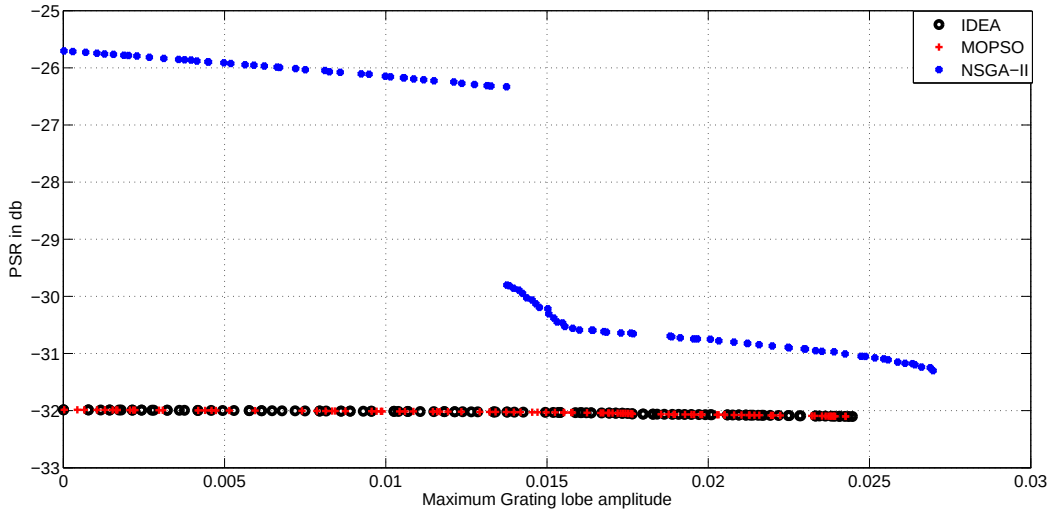

Figure 5.2: Pareto front obtained for $T_p\Delta f = [2, 10]$ and $c = [2, 5]$

below the main lobe level. on the other hand, MOPSO and IDEA both gives the peak side lobe amplitude of 32.6 dB. For maximum grating lobe amplitude to be not more than -40 dB below the main lobe level, there is an improvement of 0.8 dB in the peak side lobe amplitude. For maximum grating lobe amplitude to be -34 dB below the main lobe level (maximum amplitude of grating lobe to below 0.02), the peak side lobe given by NSGA-II, MOPSO (and IDEA) is -32.4 dB and -32.6 dB below the main lobe level. In this case the improvement in peak

side level is of just 0.2 dB

Figure 5.2 depicts the Pareto front obtain for $T_p\Delta f = [2,10]$ and $c = [2,5]$. In this result also, the Pareto front of IDEA and MOPSO is better as compare to NSGA-II for both the objective functions. From Figure 5.2, we can say that Pareto front of IDEA and MOPSO is almost same. For complete nullification of grating lobe, the maximum amplitude of side lobe is given by NSGA-II algorithm is -25.7 dB below the main lobe level. For the same case MOPSO and IDEA gives maximum side lobe -32 dB below the main lobe level. So the result obtained by IDEA and MOPSO is better than NSGA-II. IDEA (and MOPSO) provides an improvement of 6.3 dB in the maximum side lobe amplitude. For maximum grating lobe amplitude to be not more than -40 dB below the main lobe level (maximum amplitude of grating lobe to below 0.01), NSGA-II gives peak side lobe amplitude to -26.0 dB below the main lobe level. on the other hand, MOPSO and IDEA both gives the peak side lobe amplitude of 32.0 dB. For maximum grating lobe amplitude to be not more than -40 dB below the main lobe level, there is an improvement of 6.0 dB in the peak side lobe amplitude. For maximum grating lobe amplitude to be -34 dB below the main lobe level (maximum amplitude of grating lobe to below 0.02), the peak side lobe given by NSGA-II, MOPSO(and IDEA) is -31.0 dB and -32.0 dB below the main lobe level. In this case the improvement in peak side level is of 1.0 dB

Although from Figure 5.1 and 5.2, we can say that the Pareto front obtained by MOPSO and IDEA algorithm is almost same but to decide which algorithm is better we have to compare them in terms of some mathematical quantity. To compare them we use hyper-volume metrics. This metrics was introduced in Section 4.6.1.

To calculate the hypervolume metrics the reference point is chosen as $W = [0.05, -25]$. The hypervolume obtained is $0.3644, 0.3789$ and 0.3801 for NSGA-II, MOPSO and IDEA algorithm respectively. These values are obtained for the decision variable range $T_p\Delta f = [2,10]$ and $c = [2,10]$. From this metrics we can say that the Pareto front obtained by IDEA algorithm occupies more space than others. So Pareto front obtained by IDEA is better. For the decision variable range

Table 5.1: Performance metrics Obtain using MOO Algorithms for Problem-1

Performance metrics	Parameters		Hypervolume		
	$T_p\Delta f$	c	NSGA-II	MOPSO	IDEA
Hypervolume	$[2,10]$	$[2,10]$	0.3644	0.3789	**0.3801**
	$[2,10]$	$[2,5]$	0.2349	0.3532	**0.3533**
	$[5,30]$	$[2,10]$	0.3332	0.3273	**0.3335**

$T_p\Delta f = [2,10]$ and $c = [2,5]$ hypervolume for NSGA-II, MOPSO and IDEA is $0.2349, 0.3532$ and 0.3533 respectively. Hypervolume of Pareto front obtained by IDEA is more than other two algorithm, so we can say that result obtained by IDEA is better. This statement is also true for $T_p\Delta f = [5,30]$ and $c = [2,10]$, since hypervolume is large for IDEA algorithm.

To support the result obtained by optimization algorithms explained in chapter 4, we plot the ACF of SFPT by taking the parameter value obtained from Pareto front and verify the result given by optimization algorithms. For complete suppression of grating lobe, the value of $T_p\Delta f$ and c obtained by NSGA-II is 2 and 5 respectively. The plot of ACF of SFPT for these parameter is shown in Figure 5.3. In this figure the null of $|R_1(\tau)|$, coincide with the maximum value point of $|R_2(\tau)|$. The null of $|R_1(\tau)|$ and maximum of $|R_2(\tau)|$ can be seen at $\tau/T_p = 0.5$, which the location where grating lobe is below -60 dB. In the magnitude plot of $|R(\tau)|$ zero grating lobe can be observed around $\tau/T_p = 0.5$. The value of PSR obtained by, in this case is 30.8315 dB below the main lobe level, as given by NSGA-II algorithm.

For zero grating lobe amplitude, the value of $T_p\Delta f$ and c obtained by MOPSO and IDEA algorithm is 3 and 5 respectively. The plot of ACF of SFPT for these parameter is shown in Figure 5.4. For this set of parameter value, the null of $|R_1(\tau)|$, coincide with the maximum value point of $|R_2(\tau)|$ at $\tau/T_p = 0.36$. At this point the amplitude of grating lobe goes below -60 dB. The PSR obtained is 31.9889 dB below the main lobe level as given by the MOPSO and IDEA algorithm.

The parameter obtained by optimization algorithms for maximum grating lobe amplitude to be below 40 dB from main lobe are $T_p\Delta f = 2$, $c = 5.12$ and $T_p\Delta f =$

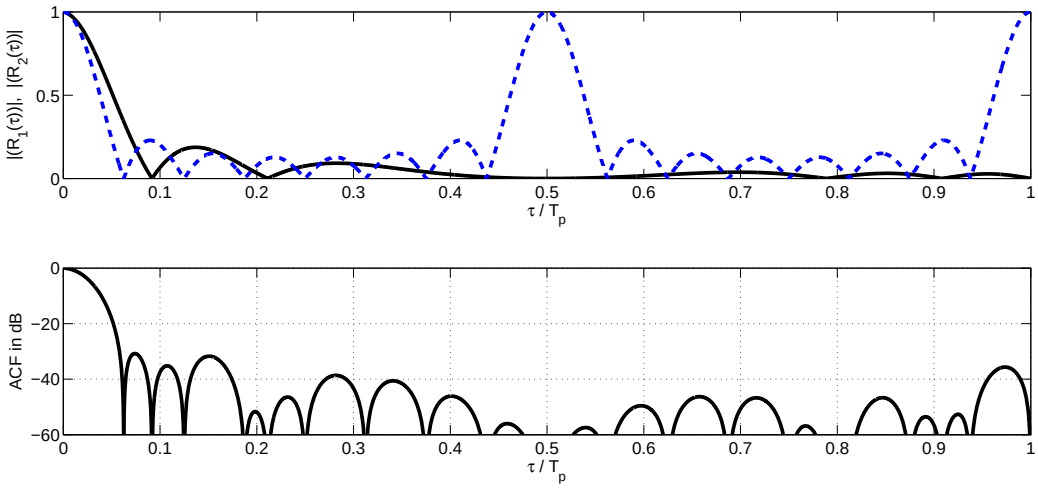

Figure 5.3: ACF plot of SFPT for $F_1 = 0$. Parameter of SFPT are obtained from NSGA-II algorithm. $T_p\Delta f = 2$, $c = 5$ and $T_pB = 12$. Top shows $|R_1(\tau)|$ by solid line and $|R_2(\tau)|$ by dashed line. Bottom shows ACF in dB

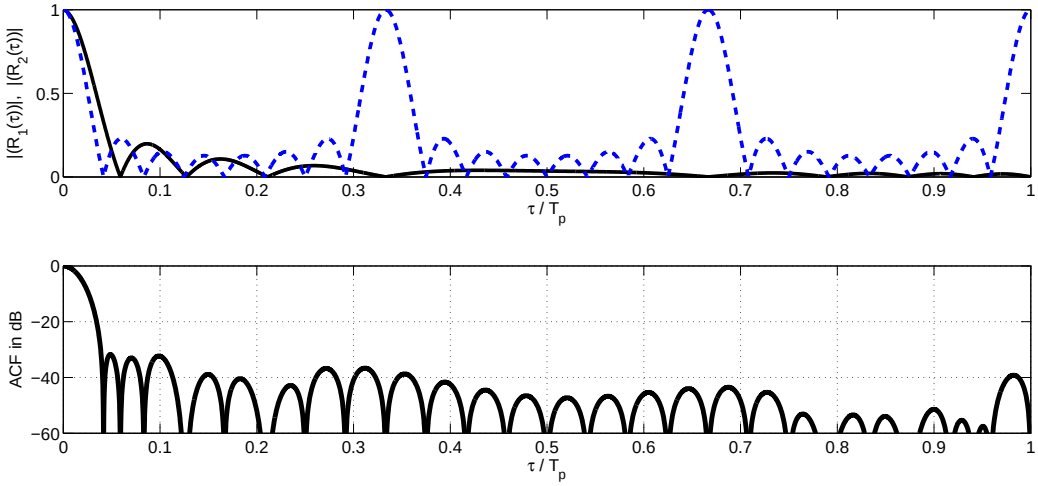

Figure 5.4: ACF plot of SFPT for $F_1 = 0$. Parameter of SFPT are obtained from MOPSO Algorithm. $T_p\Delta f = 3$, $c = 5$ and $T_pB = 18$. Top shows $|R_1(\tau)|$ by solid line and $|R_2(\tau)|$ by dashed line. Bottom shows ACF in dB

2.93, $c = 5.06$for NSGA-II and MOPSO algorithm respectively. The parameters value given IDEA and MOPSO is same for this case. The plot of ACF for these value are shown in Figure 5.5 and 5.6. In Figure 5.5 the maximum grating lobe amplitude $F_1 = 0.01$ can be observed around $\tau/T_p = 0.5$. In Figure 5.6 same point can be observed around $\tau/T_p = 0.36$. The peak side lobe can be observed around

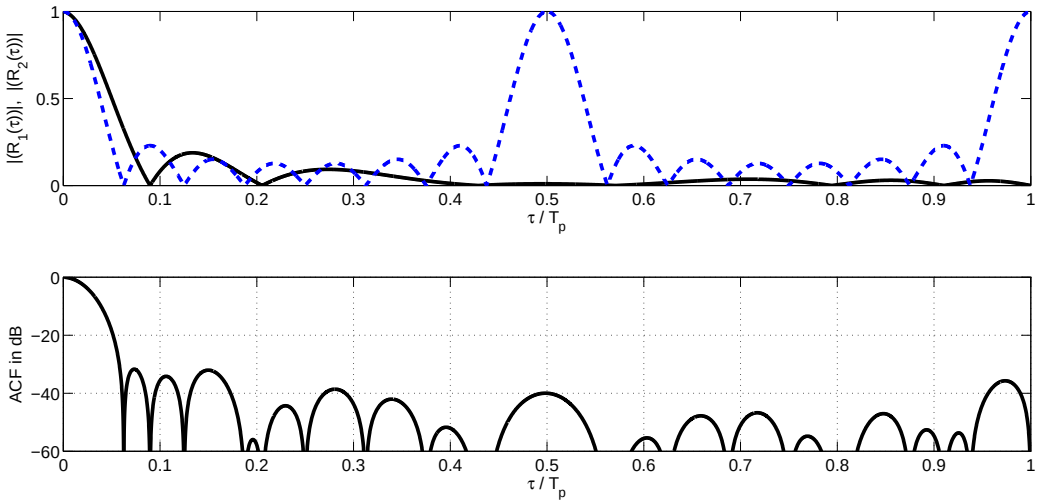

Figure 5.5: ACF plot of SFPT for $F_1 = 0.01$. Parameter of SFPT are obtained from NSGA-II Algorithm. $T_p\Delta f = 2$, $c = 5.12$ and $T_pB = 12.24$. Top shows $|R_1(\tau)|$ by solid line and $|R_2(\tau)|$ by dashed line. Bottom shows ACF in dB

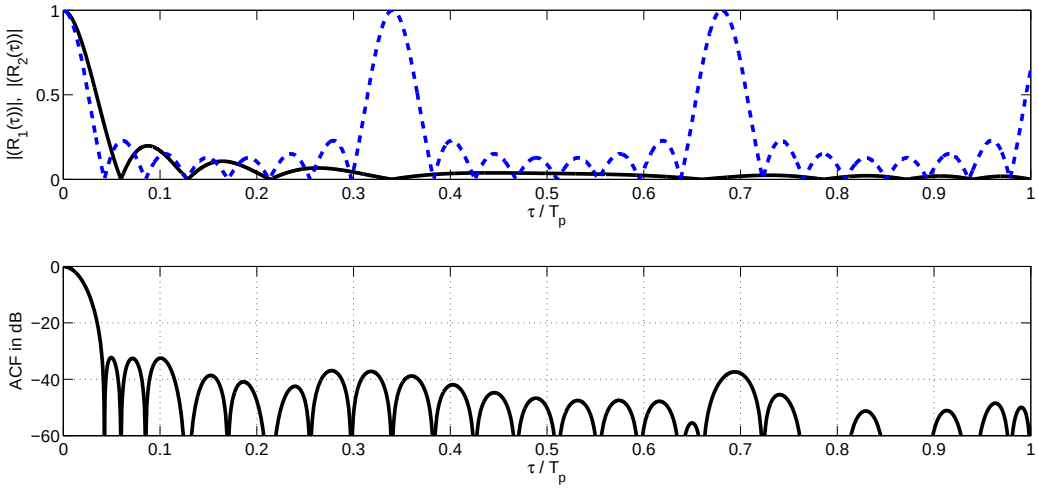

Figure 5.6: ACF plot of SFPT for $F_1 = 0.01$. Parameter of SFPT are obtained from MOPSO Algorithm. $T_p\Delta f = 2.93$, $c = 5.06$ and $T_pB = 17.75$. Top shows $|R_1(\tau)|$ by solid line and $|R_2(\tau)|$ by dashed line. Bottom shows ACF in dB

mainlobe. The amplitude of peak side lobe in Figure 5.5 is 31.6869 and in Figure 5.6 is 32.1971, which is nearly equal to the result obtained in Figure 5.1.

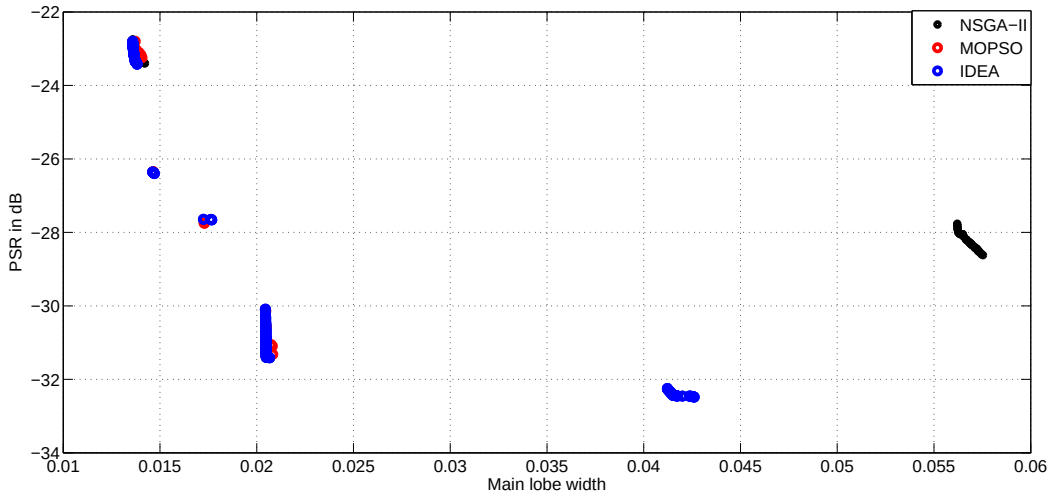

Figure 5.7: Pareto front obtained for $T_p\Delta f = [2,10]$ and $c = [2,10]$

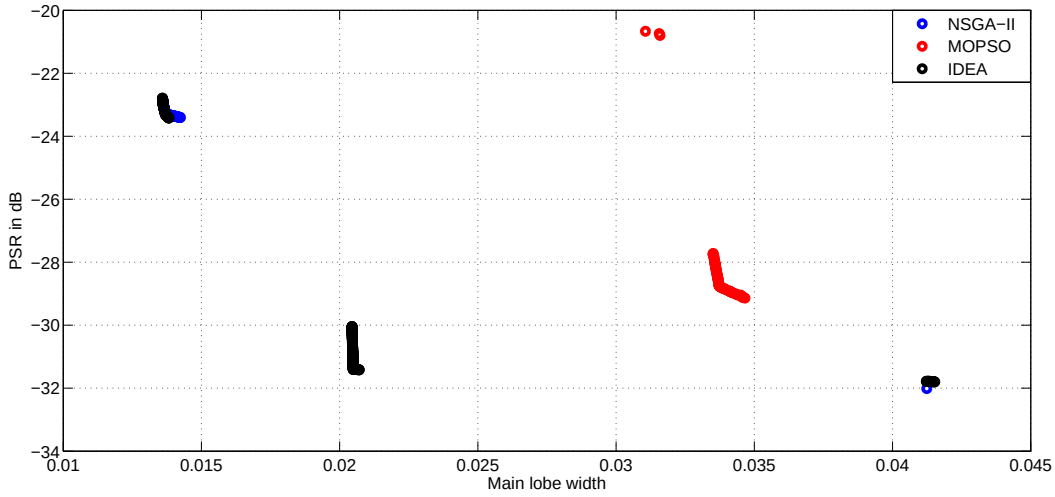

Figure 5.8: Pareto front obtained for $T_p\Delta f = [2,10]$ and $c = [2,5]$

5.2 Simulation Results for Problem-2

The Pareto front obtained using NSGA-II, MOPSO and IDEA, for problem-2 is shown in Figure 5.7, 5.8. Figure 5.7 shows the Pareto front obtain for $T_p\Delta f = [2,10]$ and $c = [2,10]$. Figure 5.8 shows the Pareto front obtain for $T_p\Delta f = [2,10]$ and $c = [2,5]$. From the figures we can observe that the Pareto front obtained for problem-2 is not continuous like problem-1. In Figure 5.7, we can see that

MOPSO algorithm is failed to find the required number of nondominated solutions. From figure it is evident that the solutions obtained by IDEA algorithm are dominates the solutions obtained by NSGA-II and MOPSO algorithm. Also the IDEA gives more diverse solution than other two algorithm.

In Figure 5.8, MOPSO algorithm is able to find many nondominated solutions, but nearly all the solutions are placed at one place. Same thing is also applicable for NSGA-II as well. Again, from Figure 5.8, we can conclude that the result obtained by IDEA dominates the solutions obtained by NSGA-II and MOPSO algorithm. So we can say that the IDEA algorithm is better than the other two algorithm.

5.3 Conclusion

In this chapter, we present the MATLAB simulation for problem-1 and 2 for different variable range. From the obtained result, we can say that obtained Pareto front by IDEA algorithm is better than the Pareto front obtained by NSGA-II algorithm and either equal or better than that of obtained by MOPSO.

Chapter 6

Conclusion and Future Work

Conclusion

Future Work

Chapter 6

Conclusion and Future Work

6.1 Conclusion

In This work, we aims to find the optimized parameter of stepped frequency pulse train for side lobe and grating lobe suppression. We have used three multi-objective optimization algorithms to find the optimized parameters of stepped frequency pulse train. We have taken two problem for optimization. In first problem our objective is to minimize grating lobe and side lobe with constraint of overall increase in bandwidth of signal. In second problem, we aims to minimize the main lobe width, which improves the resolution. second objective remain same as in problem-1. constraints for this problem is reduction of maximum grating lobe below a predefined level and increase in bandwidth. From the simulation result we can conclude that for problem-1, the Pareto front obtained by IDEA algorithm is better than obtained by NSGA-II algorithm and seems to be equal to the Pareto front obtained by MOPSO. If we compare the area covered by solution front (hyper volume metrics), from a reference point, then we can say that IDEA is marginally better than the other two algorithm. Based on this metric we can conclude that the Pareto front obtained by IDEA is more diversify and has better Convergence as compare to other two algorithms. For problem-2, none of the algorithm is able to give us the continuous Pareto front but from the obtained we can conclude that the Pareto front obtained by IDEA, dominated the Pareto front obtained by other two algorithms. So overall we can say that IDEA algorithm is better for the problems used in this work for optimization.

6.2 Future Work

In this work we have used Multi-objective optimization techniques to find the optimized parameter of stepped frequency pulse train. Since the true Pareto front of the problems is not known, so we can not the obtained result is the best, we cant get. To overcome this problem, we will use Convex Optimization technique in future to find the optimized parameter. Convex Optimization technique use mathematics to find optimized parameter, so we will get the best result. We will also used the problem formulated here to OFDM radar for pulse compression. We also aims to to FPGA implementation of pulse compression system. In the pulse compression system, we will used the obtained result, from this work, and verify our result.

Bibliography

[1] M. I. Skolnik, *Introduction to radar Systems*. Tata Mcgraw Hill, 2001.

[2] B. R. Mahafza, *Radar systems analysis and design using MATLAB*. CRC press, 2002.

[3] C. Cook, *Radar signals: An introduction to theory and application*. Elsevier, 2012.

[4] N. Levanon and E. Mozeson, *Radar signals*. John Wiley & Sons, 2004.

[5] S. Salemian, M. Jamshihi, and A. Rafiee, "Radar pulse compression techniques," in *Proceedings of the 4th WSEAS international conference on Applications of electrical engineering*, pp. 203–209, World Scientific and Engineering Academy and Society (WSEAS), 2005.

[6] Y. K. Chan, M. Y. Chua, and V. C. Koo, "Sidelobes reduction using simple two and tri-stages non linear frequency modulation (nlfm)," *Progress In Electromagnetics Research*, vol. 98, pp. 33–52, 2009.

[7] J. Johnston and A. Fairhead, "Waveform design and doppler sensitivity analysis for nonlinear fm chirp pulses," in *IEE Proceedings F (Communications, Radar and Signal Processing)*, vol. 133, pp. 163–175, IET, 1986.

[8] A. W. Rihaczek, *Principles of high-resolution radar*. McGraw-Hill New York, 1969.

[9] N. Levanon and E. Mozeson, "Nullifying acf grating lobes in stepped-frequency train of lfm pulses," *Aerospace and Electronic Systems, IEEE Transactions on*, vol. 39, no. 2, pp. 694–703, 2003.

[10] D. E. Maron, "Non-periodic frequency-jumped burst waveforms," in *Proceedings of the IEE International Radar Conference*, pp. 484–488, London, Oct, 1987.

[11] D. E. Maron, "Frequency-jumped burst waveforms with stretch processing," in *Radar Conference, Record of the IEEE 1990 International*, pp. 274–279, 1990.

[12] D. J. Rabideau, "Nonlinear synthetic wideband waveforms," in *Radar Conference, 2002. Proceedings of the IEEE*, pp. 212–219, IEEE, 2002.

[13] I. Gladkova and D. Chebanov, "Suppression of grating lobes in stepped-frequency train," in *Radar Conference, 2005 IEEE International*, pp. 371–376, IEEE, 2005.

[14] K. Deb, A. Pratap, S. Agarwal, and T. Meyarivan, "A fast and elitist multiobjective genetic algorithm: Nsga-ii," *Evolutionary Computation, IEEE Transactions on*, vol. 6, no. 2, pp. 182–197, 2002.

[15] A. K. Sahoo and G. Panda, "A multiobjective optimization approach to determine the parameters of stepped frequency pulse train," *Aerospace science and technology*, vol. 24, no. 1, pp. 101–110, 2013.

[16] V. Kumar and A. K. Sahoo, "Grating lobe and sidelobe supression using multi-objective optimization techniques," in *International Conference on Communication and Signal Processing*, pp. 246–250, 2015.

[17] C. A. C. Coello, G. T. Pulido, and M. S. Lechuga, "Handling multiple objectives with particle swarm optimization," *Evolutionary Computation, IEEE Transactions on*, vol. 8, no. 3, pp. 256–279, 2004.

[18] N. Srinivas and K. Deb, "Muiltiobjective optimization using nondominated sorting in genetic algorithms," *Evolutionary computation*, vol. 2, no. 3, pp. 221–248, 1994.

[19] T. Ray, H. K. Singh, A. Isaacs, and W. Smith, "Infeasibility driven evolutionary algorithm for constrained optimization," in *Constraint-handling in evolutionary optimization*, pp. 145–165, Springer, 2009.

[20] H. K. Singh, A. Isaacs, T. T. Nguyen, T. Ray, and X. Yao, "Performance of infeasibility driven evolutionary algorithm (idea) on constrained dynamic single objective optimization problems," in *Evolutionary Computation, 2009. CEC'09. IEEE Congress on*, pp. 3127–3134, IEEE, 2009.

[21] H. K. Singh, A. Isaacs, T. Ray, and W. Smith, "Infeasibility driven evolutionary algorithm (idea) for engineering design optimization," in *AI 2008: Advances in Artificial Intelligence*, pp. 104–115, Springer, 2008.

[22] J. Kenndy and R. Eberhart, "Particle swarm optimization," in *Proceedings of IEEE International Conference on Neural Networks*, vol. 4, pp. 1942–1948, 1995.

[23] C. A. Coello Coello and M. S. Lechuga, "Mopso: A proposal for multiple objective particle swarm optimization," in *Evolutionary Computation, 2002. CEC'02. Proceedings of the 2002 Congress on*, vol. 2, pp. 1051–1056, IEEE, 2002.

[24] J. D. Knowles and D. W. Corne, "Approximating the nondominated front using the pareto archived evolution strategy," *Evolutionary computation*, vol. 8, no. 2, pp. 149–172, 2000.

[25] E. Zitzler and L. Thiele, "Multiobjective optimization using evolutionary algorithmsa comparative case study," in *Parallel problem solving from naturePPSN V*, pp. 292–301, Springer, 1998.

[26] E. Zitzler and L. Thiele, "Multiobjective evolutionary algorithms: a comparative case study and the strength pareto approach," *evolutionary computation, IEEE transactions on*, vol. 3, no. 4, pp. 257–271, 1999.

[27] S. Jiang, Y.-S. Ong, J. Zhang, and L. Feng, "Consistencies and contradictions of performance metrics in multiobjective optimization," 2014.

[28] K. Deb, S. Agrawal, A. Pratap, and T. Meyarivan, "A fast elitist non-dominated sorting genetic algorithm for multi-objective optimization: Nsga-ii," *Lecture notes in computer science*, vol. 1917, pp. 849–858, 2000.

[29] S. Koziel and Z. Michalewicz, "Evolutionary algorithms, homomorphous mappings, and constrained parameter optimization," *Evolutionary computation*, vol. 7, no. 1, pp. 19–44, 1999.

[30] K. Deb, A. Pratap, and T. Meyarivan, "Constrained test problems for multi-objective evolutionary optimization," in *Evolutionary Multi-Criterion Optimization*, pp. 284–298, Springer, 2001.

[31] I. Gladkova and D. Chebanov, "Grating lobes suppression in stepped-frequency pulse train," *Aerospace and Electronic Systems, IEEE Transactions on*, vol. 44, no. 4, pp. 1265–1275, 2008.

[32] C. A. C. Coello and G. B. Lamont, *Applications of multi-objective evolutionary algorithms*, vol. 1. World Scientific, 2004.

[33] S. Boukeffa, Y. Jiang, and T. Jiang, "Sidelobe reduction with nonlinear frequency modulated waveforms," in *Signal Processing and its Applications (CSPA), 2011 IEEE 7th International Colloquium on*, pp. 399–403, IEEE, 2011.

[34] S. S. Y. M. Thin Thin Mar, "Pulse compression method for radar signal processing," *International Journal of Science and Engineering Applications (IJSEA)*, vol. 3, no. 2, pp. 31 – 35, 2014.